REPORT DOCUMENTATION PAGE

Form Approved
OMB No. 0704-0188

1. REPORT DATE *(DD-MM-YYYY)*	**2. REPORT TYPE**	**3. DATES COVERED** *(From - To)*
28 August 2012	Journal Article	Jan – Aug 2012

4. TITLE AND SUBTITLE
Hansen Solubility Parameters for Octahedral Oligomeric Silsesquioxanes

5a. CONTRACT NUMBER
In-House

5b. GRANT NUMBER

5c. PROGRAM ELEMENT NUMBER

6. AUTHOR(S)
Andrew J. Guenthner, Kevin R. Lamison, Lisa M. Lubin,
Timothy S. Haddad, Joseph M. Mabry

5d. PROJECT NUMBER

5e. TASK NUMBER

5f. WORK UNIT NUMBER
Q0AD

7. PERFORMING ORGANIZATION NAME(S) AND ADDRESS(ES)
Air Force Research Laboratory (AFMC)
AFRL/RQRP
10 E. Saturn Blvd
Edwards AFB CA 93524-7401

8. PERFORMING ORGANIZATION REPORT NO.

9. SPONSORING / MONITORING AGENCY NAME(S) AND ADDRESS(ES)
Air Force Research Laboratory (AFMC)

AFRL/RQR
5 Pollux Drive
Edwards AFB CA 93524-7048

10. SPONSOR/MONITOR'S ACRONYM(S)

11. SPONSOR/MONITOR'S REPORT NUMBER(S)
AFRL-RZ-ED-JA-2012-135

12. DISTRIBUTION / AVAILABILITY STATEMENT
Approved for public release, distribution unlimited. (PA# 12306)

13. SUPPLEMENTARY NOTES

14. ABSTRACT

The Hansen Solubility Parameters (HSP) for several polyhedral oligomeric silsesquioxane (POSS) compounds were successfully determined, demonstrating the applicability of the HSP approach for selected types of organic–inorganic compounds. As commonly practiced with organic polymers, a set of simple "pass/fail" tests for complete solubility at a fixed concentration (100 mg/mL) was conducted for an array of five octameric POSS compounds, octa(phenethyl), octa(styrenyl), octa(isobutyl), octakis(hexafluoroisobutyl), and (1-naphthyl)heptaphenyl), and 45 test solvents. Group contributions for the octameric POSS cage were determined using three different approaches, which produced similar results. The best cage contribution estimate for the dispersive, polar, and hydrogen-bonding components δD, δP,, and δH of the total solubility parameter was determined to be δD = 22 (J/cc)1/2, δP = 19 (J/cc)1/2, and δH = 15 (J/cc)1/2, with an estimated uncertainty of approximately 5 (J/cc)1/2. The utility of the HSP approach was demonstrated by successfully identifying mixtures of poor solvents that provided significantly enhanced solubility for octa(isobutyl) POSS, and by successfully estimating the HSP of octakis(trifluoropropyl) POSS from group contributions derived solely from aromatic POSS compounds.

15. SUBJECT TERMS

16. SECURITY CLASSIFICATION OF:			**17. LIMITATION OF ABSTRACT**	**18. NUMBER OF PAGES**	**19a. NAME OF RESPONSIBLE PERSON**
					Joseph M. Mabry
a. REPORT	**b. ABSTRACT**	**c. THIS PAGE**	SAR	50	**19b. TELEPHONE NO** *(include area code)*
Unclassified	**Unclassified**	**Unclassified**			661-275-5857

Hansen Solubility Parameters for Octahedral Oligomeric Silsesquioxanes

Andrew J. Guenthner[1], Kevin R. Lamison[2], Lisa M. Lubin[2], Timothy S. Haddad[2], Joseph M. Mabry[1]*

[1]Propulsion Directorate, Air Force Research Laboratory, Edwards AFB, CA 93524

[2]ERC Incorporated, Air Force Research Laboratory, Edwards AFB, CA 93524

*andrew.guenthner@edwards.af.mil

RECEIVED DATE

Abstract

The Hansen Solubility Parameters (HSP) for several Polyhedral Oligomeric SilSesquioxane (POSS) compounds were successfully determined, demonstrating the applicability of the HSP approach for selected types of organic-inorganic compounds. As commonly practiced with organic polymers, a set of simple "pass/fail" tests for complete solubility at a fixed concentration (100 mg/mL) was conducted for an array of five octameric POSS compounds, octa(phenethyl), octa(styrenyl), octa(*iso*butyl), octakis(hexafluoro*iso*butyl), and (1-naphthyl)heptaphenyl), and 45 test solvents. Group contributions for the octameric POSS cage were determined using three different approaches, which produced similar results. The best cage contribution estimate for the dispersive, polar, and hydrogen-bonding components δ_D, $\delta_{P,}$, and δ_H of the total solubility parameter was determined to be δ_D = 22 $(J/cc)^{1/2}$, δ_P = 19 $(J/cc)^{1/2}$, and δ_H = 15 $(J/cc)^{1/2}$, with an estimated uncertainty of approx. 5 $(J/cc)^{1/2}$. The utility of the HSP approach was demonstrated by successfully identifying mixtures of poor solvents that provided

significantly enhanced solubility for octa(*iso*butyl) POSS, and by successfully estimating the HSP of octakis(trifluoropropyl) POSS from group contributions derived solely from aromatic POSS compounds.

1. Introduction

Over the past few decades, Hansen Solubility Parameters (HSP) have achieved a high level of prominence in the coatings industry as a practical tool for estimating a variety of thermodynamic and transport properties in polymer systems.[1-4] An advantage of the HSP approach over the simpler one-component Hildebrand solubility parameter theory is that the HSP approach enables the identification of mixtures of non-solvents that, when combined in the proper ratio, become good solvents for difficult to dissolve polymers.[5] The adoption of the HSP approach to the more general problem of finding sets of polymers and/or small-molecule fluids that display desired thermodynamic interaction characteristics, whether favorable or unfavorable, has saved countless hours of trial and error in gas separation membranes,[6] drug delivery,[7-9] and nanocomposite[10-15] applications. It is, therefore, virtually certain that successful efforts aimed at expanding the range of applicability of Hansen Solubility Parameters will generate numerous very substantial positive impacts across a wide variety of industries.

Polyhedral Oligomeric SilSesquioxanes (POSS)[16] are a family of inorganic/organic core/shell nanostructures possessing molecular weight values on the order of 1000 g/mol, in which the core consists of a silsesquioxane cage with the formula $(SiO_{1.5})_n$, where n is generally between 8 and 14. The shell consists of n organic functional groups originating at each Si atom on a cage vertex. Cages are generally categorized according to the bonding type and number of silicon atoms that comprise each vertex. The functionality may vary from one organic group to another, although the most commonly used compounds feature octameric cages with identical, simple functional groups.

Since their commercialization in the late 1990s, POSS compounds have found a large variety of uses, particularly as modifiers for polymers and inorganic fillers in the medical,[17] aerospace,[18] and electronics industries,[19] where they serve as processing aids for high-temperature thermoplastics, dispersion and

compatibilization agents, and thermal and electrical insulation enhancers. The inorganic core is both mechanically robust, resistant to oxidation, and thermally stable, and the ability to synthesize a variety of peripheral groups makes the tailoring of properties fairly straightforward. Despite the many applications for POSS compounds that involve thermodynamic compatibility and mixing, there have been few systematic comparative attempts to quantify POSS solubility in common organic solvents.[20, 21]

More significant effort, however, has been devoted to exploring the solubility of inert POSS compounds in polymers.[16, 19] There have been numerous reports of good compatibility between certain POSS compounds and selected polymers, e.g., octakis(2-phenylethyl), referred to as octa(phenethyl), POSS and either polystyrene[22] or polyvinyl chloride.[23] However, in many cases, the reported solubility of POSS compounds in polymers of interest is quite limited. Therefore, there is a clear need for a rational approach to determine the solubility and thermodynamic interactions of POSS compounds with both solvents and polymers.

Despite the obvious need, there has been only a small amount of published work to date on the solubility parameters for POSS compounds. Recent work reported by the Morgan group[24-26] has focused on determination of the Hildebrand solubility parameters of POSS compounds with partial success in predicting polymer compatibility. Other recent work by Lim et al.[27, 28] has shown that calculation of the HSP for the peripheral arms of POSS compounds (ignoring the cage entirely) provides limited comparative insight into polymer compatibility as well. In most cases, the Hansen Solubility Parameter approach has been limited to purely organic compounds, with only a few investigations performed for inorganic groups[29, 30] (mainly in the context of nanoparticles or surfaces[13-15, 31-35]), or for organic/inorganic polymers, such as polysiloxanes[36-38] and polyphosphazines.[39] The size and even shape of POSS molecules, however, would not be expected to preclude the determination of HSP because the HSP approach has been successfully applied to compounds such as fullerenes,[12, 40] asphaltenes,[41-44] and bitumen[45, 46] that are intermediates between small molecules and polymer chains. Though for nanoparticles in general, one would expect the solubility parameters to reflect the surface, rather than bulk composition, for POSS compounds, the central cage is at least partially accessible to

surrounding molecules, and the overall issue of solvent accessibility is similar to those encountered for many types of polymers. In short, given the many benefits that will accrue from successful application of HSP to POSS compounds, the subject is worth considerable further investigation.

Herein we report the results of our efforts to determine Hansen Solubility Parameters for selected POSS compounds. We found that, for an initial group of five POSS compounds, simple solubility testing of the type carried out for polymers was adequate for the determination of the HSP values. We further found that the consistency of the results was of the same quality encountered for most polymer systems, and that there appeared to be no fundamental disadvantage associated with POSS compounds as a group. Additional analysis of these HSP values allowed us to investigate the possibility of assigning a group contribution to the octameric cage, where we determined that, although a reasonably consistent set of parameters could be obtained for many compounds, the issue of cage accessibility may complicate matters more than in a typical polymer. Our results represent an important extension of HSP in the realm of inorganic/organic materials, a significant but logical step forward that is certain to bring substantial benefits to the ever growing array of applications in which POSS compounds are featured prominently.

2. Experimental

2.1 Materials. Octa(phenethyl) POSS, octa(styrenyl) POSS, octakis(hexafluoro*iso*butyl) POSS, and (1-naphthyl)heptaphenyl POSS were synthesized at AFRL. Octa(*iso*butyl) POSS was obtained from Hybrid Plastics (Hattiesburg, MS). The chemical structure of these compounds is given in Figure 1. A large amount of data is available for the octa(*iso*butyl) compound,[16] with limited data available for the octa(phenethyl),[22, 23, 47-53] octa(styrenyl),[52, 54] octakis(hexafluoro*iso*butyl),[55] and, more recently, the (1-naphthyl)heptaphenyl[21] compounds, respectively. The set of 45 solvents used in the study were obtained from a variety of commercial sources. Most were of technical grade, and all were used in as-received condition. All are listed in Supporting Information.

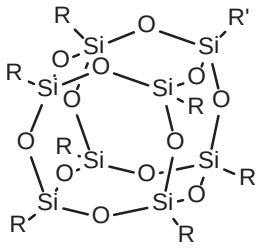

1a: R, R' = -CH_2CH_2-C_6H_5
1b: R,R' = -CH=CH-C_6H_5
1c: R,R' = -$CH_2(CH)(CH_3)_2$
1d: R,R' = -$CH_2(CH)(CF_3)_2$
1e: R = -C_6H_5; R' = 1-naphthyl

Figure 1: Chemical structure of POSS compounds for which HSP were determined.

2.2 Test Procedures. For each of the tests reported herein, 50 mg of the POSS compound was placed in a clean 5 mL glass vial along with 0.5 mL of the selected solvent. The tightly closed vials were then stirred for two minutes and checked for dissolution. When complete dissolution did not occur, the vials were allowed to stand for up to one hour. The tests were then rated as follows: "Pass" indicated complete dissolution within two minutes; "Pass –" indicated complete dissolution within one hour but not within two minutes (in these cases, most of the solute dissolved initially and extra time was required to achieve complete dissolution, an indication of near saturation given the low molecular weight of the POSS compounds); "Fail +" indicated that significant but incomplete dissolution occurred; "Fail" indicated that little or no dissolution was observed. Note that, in general, "Pass –" was treated as "Pass" and "Fail +" as "Fail".

Analysis Procedures. The primary goal of the analysis for a given POSS compound was to provide a best estimate of the dispersive (δ_D), polar (δ_P), and hydrogen bonding (δ_H) components of the Hansen Solubility Parameter. In addition, some indication of the uncertainty in the HSP values, as well as an estimate of the "radius of interaction" (R_0) that defines the expected boundary in "HSP space" between "good" and "poor" solvents, was also desired. More information on these concepts can be found in the work by Hansen.[1]

The basic approach was to maximize the goodness of fit of the data set to the "sphere of solubility" described by Hansen,[1] based on the pass/fail ratings (here denoted as "$test_i$" and the associated HSP ($\delta_{D\text{-}S,i}$, $\delta_{P\text{-}S,i}$, $\delta_{H\text{-}S,i}$) of each solvent tested. Namely, for each instance i, a characteristic distance R_a was defined such that

$$R_{a,i} = 4 * (\delta_{D\text{-}POSS} - \delta_{D\text{-}S,i})^2 + (\delta_{P\text{-}POSS} - \delta_{P\text{-}S,i})^2 + (\delta_{H\text{-}POSS} - \delta_{H\text{-}S,i})^2 \quad (1)$$

with the criteria being

If $R_{a,i} < R_0$, then $test_i$ = "Pass." Otherwise, $_{testi}$ = "Fail"

in which $\delta_{D\text{-}POSS}$, $\delta_{P\text{-}POSS}$, $\delta_{H\text{-}POSS}$, and R_0 are adjustable parameters. The goodness of fit was determined by means of a χ^2 test, using the total fraction of tests grades as "Pass" and the total fraction of solvents for which $R_{a,i} < R_0$ to determine the distribution of expected occurrences. The procedure described above was the computational equivalent of attempting to identify the central coordinates and radius of a sphere that included all solvents with a "pass" rating but excluded all solvents with a "fail" rating, in a Cartesian space with axes given by 2 δ_D, δ_P, and δ_H.

To locate the optimal values of $\delta_{D\text{-}POSS}$, $\delta_{P\text{-}POSS}$, $\delta_{H\text{-}POSS}$, and R_0, a brute force method based on an iteratively refined search space was employed. In the first iteration, $\delta_{D\text{-}POSS}$ was varied from 15 to 20 in increments of 0.5, while $\delta_{P\text{-}POSS}$ and $\delta_{H\text{-}POSS}$ were varied from 0 to 10 in increments of 1, while R_0 was varied from 0 to 20 in increments of 0.25. The initial range represented a compromise between comprehensiveness and the need to minimize computation time, and was based on the range of the HSP noted for solvents with a rating of "pass". For every possible combination of the four parameters given the ranges and increments listed above, the χ^2 parameter was then calculated and the absolute maximum recorded. For the second iteration, the search grid was centered on the point having maximum χ^2 (with the lowest value of all other parameters used to break ties) found in the previous iteration, with the increments reduced to 0.4 for $\delta_{D\text{-}POSS}$, and 0.8 for $\delta_{P\text{-}POSS}$ and $\delta_{H\text{-}POSS}$, while the increment was maintained at 0.25 for R_0. (These values were chosen to provide conveniently divisible intervals for subsequent iterations while enabling the search space to be expanded well beyond the originally chosen boundaries if necessary.) The process was repeated two additional times, centering the grid as described previously and reducing the increment for $\delta_{D\text{-}POSS}$, $\delta_{P\text{-}POSS}$, and $\delta_{H\text{-}POSS}$ by a factor of 4 each time, while maintaining the increment for R_0. The method provided a final search resolution of 0.025 for $\delta_{D\text{-}POSS}$, 0.05 for $\delta_{P\text{-}POSS}$ and $\delta_{H\text{-}POSS}$, and 0.25 for R_0. Note that the finer spacing for $\delta_{D\text{-}POSS}$ was used to compensate for the factor of 4 in the Hansen expression (effectively, the parameter 2 $\delta_{D\text{-}POSS}$ was used as

a dimension along with $\delta_{P\text{-}POSS}$, and $\delta_{H\text{-}POSS}$ in a uniform Cartesian search grid that shrank with each iteration until the optimal center co-ordinates were identified).

Due to the highly non-linear nature of the optimization process, many possible locations in "HSP space" bounded by an irregular and even non-contiguous region can be of equal or nearly equal goodness of fit, thus it is important to obtain some estimate of uncertainty. To address this issue, we again employed a brute force method, calculating the χ^2 value for all combinations of $\delta_{D\text{-}POSS}$, $\delta_{P\text{-}POSS}$, $\delta_{H\text{-}POSS}$, and R_0 with increments of 0.05, 0.1, 0.1, and 0.25, respectively, around the optimal point identified in the final search iteration with a span of 11 increments for $\delta_{D\text{-}POSS}$, $\delta_{P\text{-}POSS}$, and $\delta_{H\text{-}POSS}$ and 41 increments for R_0. We considered χ^2 values that differed from the previously determined optimum by less than one to be representative of equivalent goodness of fit. This practice, originally suggested by E. von Meerwaal of the University of Akron, was found to work quite well in this situation. The values of every combination of $\delta_{D\text{-}POSS}$, $\delta_{P\text{-}POSS}$, and $\delta_{H\text{-}POSS}$ for which at least one value of R_0 enabled the condition for equivalent goodness of fit to be met were logged. If any of these coordinates fell on the boundary of the search region, the increments of $\delta_{D\text{-}POSS}$, $\delta_{P\text{-}POSS}$, and $\delta_{H\text{-}POSS}$ were increased in linear steps of 100% (i.e. they were first doubled from their original values, then tripled from their original values, etc.), and the entire process repeated, until no co-ordinates on the boundary of the search region met the criteria. We then calculated the centroid and radii of gyration (in each dimension) of the set of all co-ordinates that met the goodness of fit criteria, using the centroid for the finally determined values of the HSP for the given POSS compound. The R_0 values from the list of all co-ordinate combinations that met the goodness of fit criteria were averaged and reported as the final R_0 value for the POSS compound. The radii of gyration were then reported as the "characteristic uncertainty" of the measurement.

3. Results and Discussion

3.1 General Overview

Figures 2-6 depict the outcomes of the solvent testing for the octa(phenethyl) (Figure 2), octa(styrenyl) (Figure 3), octa(*iso*butyl) (Figure 4), octakis(hexafluoro*iso*butyl) (Figure 5) and (1-

naphthyl)heptaphenyl (Figure 6) POSS compounds. In each of these Figures, the axes represent the HSP with the scaling suggested by Hansen, with δ_D compressed by two. The filled symbols represent the HSP of solvents that rated "pass", while the unfilled symbols reflect the solvents that rated "fail". The spherical object represents the predicted "pass/fail" boundary, based on the calculated HSP for the individual POSS compound (the center co-ordinates of the sphere) and the calculated value of the "radius of interaction" R_0. Numerical values of the calculated HSP, R_0, characteristic uncertainties (see Experimental section for details), and data on the overall solubility have been provided in Table 1, as well as the number of failed predictions based on the relative energy difference (RED) concept,[1] in which the RED is defined as the ratio of the distance in "HSP space" between the co-ordinates of the POSS compound and the solvent to R_0, with "good" solvents expected when RED < 1 and "poor" solvents expected for RED > 1.

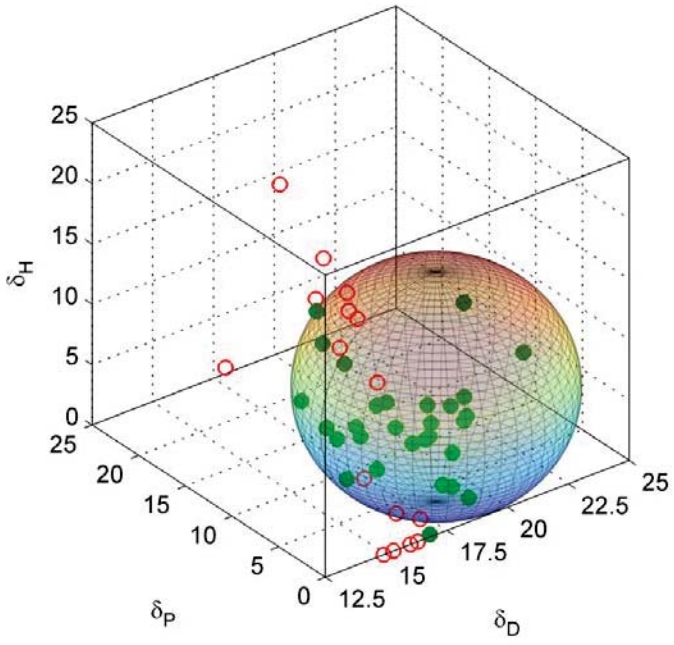

Figure 2. Results of solubility testing for octa(phenethyl) POSS. Filled symbols indicate solvents with a rating of "pass" (complete solubility at 100 mg/mL), while open symbols indicate solvents with a rating of "fail". The "sphere of solubility" that best describes the data (based on maximizing χ^2) is also shown.

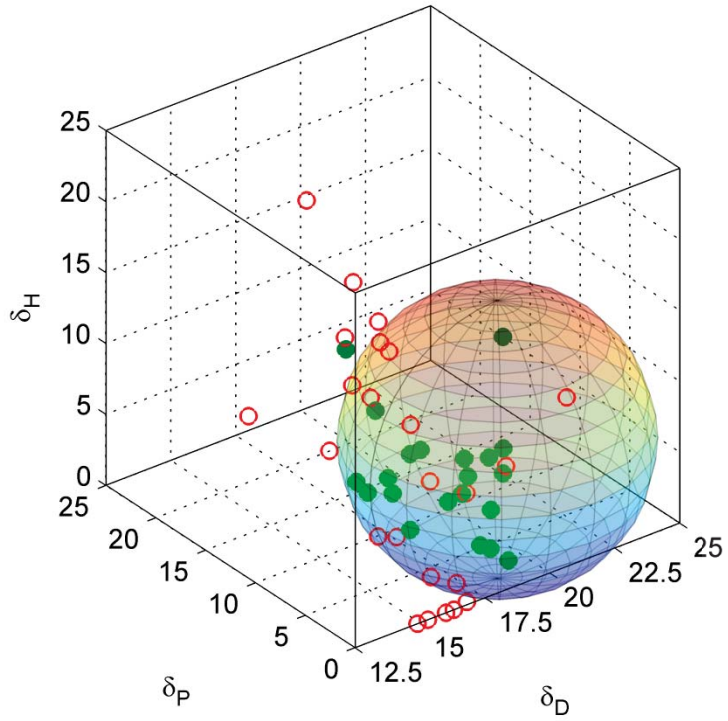

Figure 3. Results of solubility testing for octa(styrenyl) POSS, with data displayed as in Figure 2.

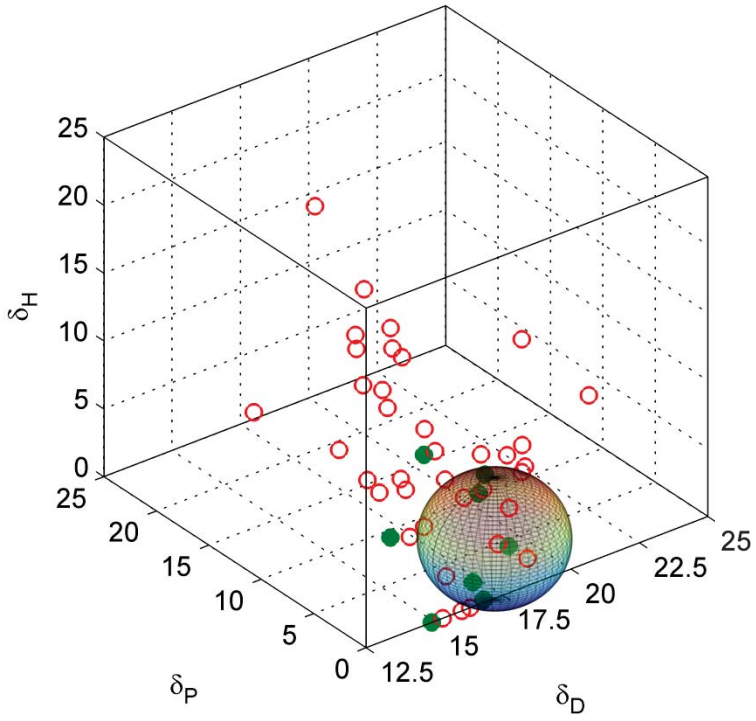

Figure 4. Results of solubility testing for octa(*iso*butyl) POSS, with data displayed as in Figure 2.

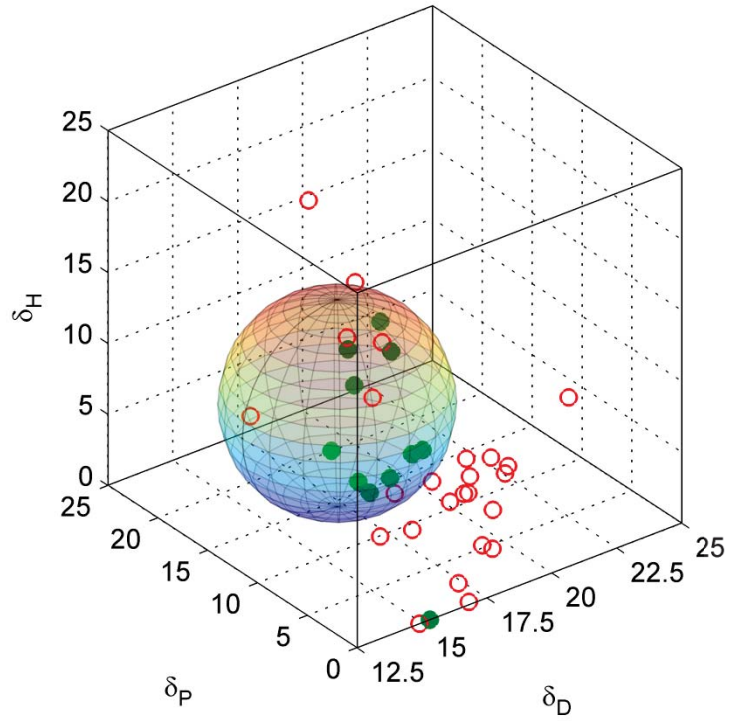

Figure 5. Results of solubility testing for octakis(hexafluoro*iso*butyl) POSS, with data displayed as in Figure 2.

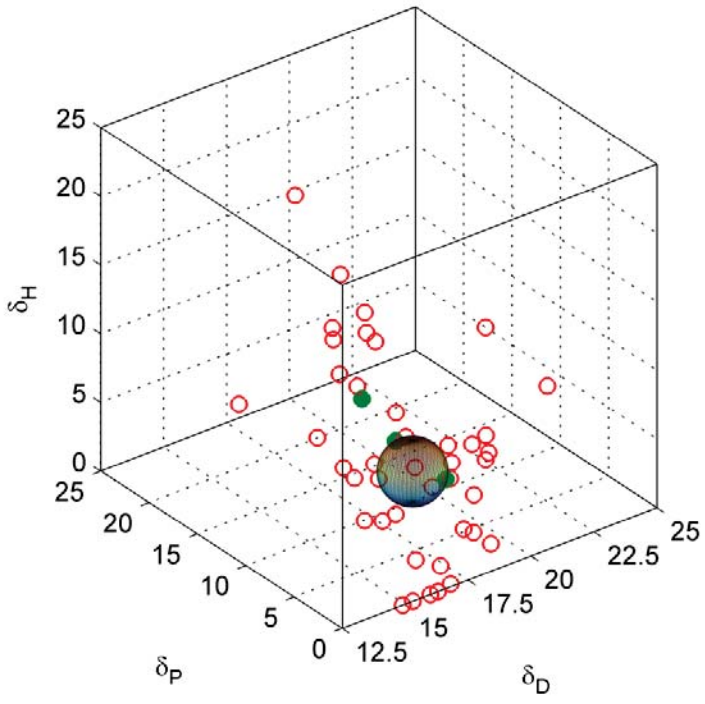

Figure 6. Results of solubility testing for (1-naphthyl)heptaphenyl POSS, with data displayed as in Figure 2.

Table 1

Estimated HSP and Selected Related Characteristics of Octameric POSS Compounds (Standard Analysis)

Name (Code)	δ_D Centroid	δ_D R_G	δ_P Centroid	δ_P R_G	δ_H Centroid	δ_H R_G	R_0	# Good / # Tested	# Anomalies
Octa(phenethyl) (PE-1)	19.9	0.4	7.4	0.5	6.3	0.6	9.8	29/45	2
Octa(styrenyl) (ST-1)	20.2	0.7	5.8	0.8	6.6	0.7	9.8	21/45	5
Octa(*iso*butyl) (IB-1)	18.0	0.1	2.1	0.2	2.7	0.3	4.3	8/45	6
Octakis(hexafluoro-*iso*butyl) (HF-1)	15.3	0.8	9.3	0.9	11.0	0.6	7.3	10/36	2
(1-naphthyl)hepta-phenyl (NP-1)	16.9	0.1	4.0	0.2	6.3	0.2	2.5	3/45	1

R_G = radius of gyration, a measure of the uncertainty

Perhaps the most important general result that can be appreciated from examination of Figures 2-6 is the level of success of the HSP approach for the POSS compounds. In general, the best fit predictions result in errors (counting both anomalous good and anomalous poor solvents) of only approx. 25%, as often as they successfully identify good solvents, whereas assigning otherwise randomly chosen guesses based only on the proportion of solvents rated "pass" for a particular compound results in about 2.5 errors for every good solvent successfully identified. In other words, the use of HSP for POSS compounds results in about a 90% reduction in time lost to trial and error.

3.2 HSP of Individual POSS Compounds

Of the POSS compounds examined, octa(phenethyl) POSS (Figure 2) proved to be the most generally soluble, achieving a rating of "pass" in 29 out of the 45 solvents tested. All but two of the passing solvents, and none of the failing solvents, lay inside a sphere of radius 9.8 centered at (δ_D, δ_P, δ_H) = (19.9, 7.4, 6.3). The two exceptions were cyclohexane and diethyl ether, which were only slightly outside the sphere. The uncertainty in the determined HSP values could be traced to a lack of non-solvents with a suitably high δ_D value, which results in less than optimal constraint on the location of the sphere of solubility. Such a lack of optimal constraint is a fairly common issue when HSP determinations are performed.

Two additional attempts to generate an octa(phenethyl) POSS solubility data set that was more easily constrained were made. First, the set of solubility tests was repeated using a concentration of 200 mg/mL, rather than 100 mg/mL, with the intent of generating fewer passing solvents and shrinking the radius of interaction. Although the number of passing solvents was reduced to 19, this approach was unsuccessful because the solvents with the highest δ_D still passed. By disproportionately eliminating solvents that helped to constrain the sphere, the uncertainties were in fact made worse. (Data for this and other "Supplemental" tests is provided in Table 2). Secondly, an additional two solvents and ten solvent mixtures (listed in Supporting Information) were chosen based on their location in "uncharted" regions of HSP space near the probable boundary of the sphere of solubility and tested at 100 mg/mL. The results were then combined with those from the original 45 solvents. The second procedure was modestly effective at further constraining the sphere of solubility. The results, as seen in Table 2, were changed little in terms of actual HSP co-ordinates. However, the uncertainties were reduced.

Table 2

Estimated HSP and Selected Related Characteristics of Octameric POSS Compounds (Supplemental Analysis)

Analysis (Code)	δ_D Centroid	δ_D R_G	δ_P Centroid	δ_P R_G	δ_H Centroid	δ_H R_G	R_0	# Good / # Tested	# Anomalies
Octa(phenethyl) @ 200 mg/mL (PE-A1)	21.6	0.5	6.2	0.2	9.9	0.4	11.8	19/45	2
Octa(phenethyl) with additional solvents and mixtures (PE-A2)	19.7	0.3	8.0	0.2	5.6	0.4	9.6	35/57	3
(1-naphthyl)hepta-phenyl @ 50 mg/mL (NP-A1)	16.9	0.1	4.0	0.2	6.3	0.2	2.5	3/45	1
(1-naphthyl)hepta-phenyl with "fail +" considered equal to "pass" (NP-A2)	18.1	0.2	8.6	0.3	6.7	0.1	4.3	7/45	2

The solubility of octa(styrenyl) POSS, a more rigid analog of octa(phenethyl) POSS, was predicted only modestly less accurately by the "spherical rule", with five exceptions (all non-solvents within the

sphere) out of 45 solvents, and with three of the exceptions exhibiting partial solubility. Though octa(styrenyl) POSS was somewhat less soluble overall (21 passing solvents) compared to octa(phenethyl) POSS, the R_0 values for octa(styrenyl) and octa(phenethyl) POSS were equivalent. The octa(styrenyl) POSS had a slightly higher δ_D value than octa(phenethyl) POSS, meaning that its calculated HSP also were made more uncertain by lack of constraints.

Though known for its good polymer compatibility characteristics,[16] octa(*iso*butyl) POSS (Figure 4) exhibited a significantly smaller radius of interaction than either octa(phenethyl) or octa(styrenyl) POSS. Though well-constrained, the solubility envelope appeared less well-defined, with six exceptions (three of each type) found. Given that only eight solvents passed (with eight also found inside the sphere), the odds that a solvent having sufficiently similar HSP to octa(*iso*butyl) POSS was, in fact, a good solvent were just over 60%. On the other hand, good solvents for octa(*iso*butyl) POSS were found at RED values (the distance to the center of the sphere divided by the radius of interaction) of 1.6. Interestingly, the anomalous poor solvents (benzene, xylenes, and phenyl acetylene) were all small aromatic hydrocarbons, while toluene was soluble at 100 mg/mL). The anomalous good solvents were n-hexane, diethyl ether, and tetrahydrofuran. While the predictive power for the HSP approach was less effective for octa(*iso*butyl) POSS than for any other compound in this study, it was still on par with test results from many organic polymers.

In order to further explore similar POSS compounds, testing was undertaken with 36 solvent candidates on octakis(hexafluoro*iso*butyl) POSS (Figure 5), a member of the class of compounds known as "fluoro POSS" that have played a key role in realizing superoleophobicity on rough surfaces.[55, 56 57] The octakis(hexafluoro*iso*butyl) POSS was in general more soluble than octa(*iso*butyl) POSS, having a larger radius of interaction. There were also just two exceptions to the "spherical rule", *iso*propanol (an anomalous poor solvent lying just inside the boundary of the sphere, note that 1-propanol and 1-butanol were good solvents and within the sphere), and n-heptane as an anomalous good solvent.

Finally, a highly aromatic POSS compound was also examined, (1-naphthyl)heptaphenyl POSS (Figure 6). Although most aromatic POSS compounds are very poorly soluble, the asymmetric

substitution pattern appears to enable at least limited solubility.[21] A total of three good solvents enabled a rudimentary estimate of the HSP for the compound, with a small radius of interaction and just one exception to the "spherical rule", albeit a crucial one: 1-methyl-2-pyrrolidone proved to be a good solvent despite having an RED value of 3.4. With only three good solvents, it is difficult to justify ignoring this anomaly on the basis of only two other data points.

In an effort to clarify the HSP for this compound, attempts were made to identify more "good" solvents to improve the robustness of the analysis. First, the non-solvents were all re-tested at a lower concentration of 50 mg/mL to try and broaden the criteria for inclusion of "good" solvents. Unfortunately, in every case for which the aromatic POSS compound failed to dissolve at 100 mg/mL, it also failed to dissolve completely at 50 mg/mL. However, in addition to the three "good" solvents (chloroform, tetrahydrofuran, and 1-methyl-2-pyrrolidone), there were four solvents in these tests that received the "fail +" rating, meaning that partial solubility was noted. Although less quantitative than the standard approach, adding these four solvents to the list of "good" solvents allowed for a more robust calculation of the HSP, with the results shown in Table 2. In this case, no poor solvents lay within the sphere of solubility, and only two good solvents (chloroform and diphenyl ether) were found outside of the sphere, in both cases by a short distance.

3.3 Estimation of Group Contribution Parameters for Octameric POSS Cages

Having identified HSP for five POSS compounds, it is reasonable to consider whether or not a systematic pattern exists with respect to the HSP of the peripheral groups. If a systematic pattern does exist, then it should be possible to identify a "group contribution" for the octameric POSS cage at the core of the five compounds studied. With such a "group contribution" in hand, it would then be possible to calculate estimated HSP for any octameric POSS compound. (Other methods based on more sophisticated computational techniques[58-64] might also be useful in estimating the HSP for POSS compounds. However, a group contribution approach would be highly valuable due to its simplicity.) It should be noted, however, that with HSP data available for only a very few compounds, any such group contribution estimates will, of necessity, be of a rough, preliminary nature.

In order to determine whether a meaningful group contribution exists, one may formally divide the cohesive energy of the POSS compounds into two parts, one arising from the cage and one arising from the peripheral arms, or

$$E_{i,POSS} = E_{i,cage} + \sum_{j=1}^{n} E_{i,jth-arm} \quad (2)$$

in which E_i represents the i^{th} cohesive energy component (dispersive, polar, or hydrogen bonding) for a system comprising the central cage and n peripheral organic groups (arms), not all of which are necessarily identical. This formal division is the simplest method that allows for modeling of a wide variety of POSS compounds. If values for $E_{i,jth\text{-}arm}$ can be calculated through existing group contribution methods, then the total component cohesive energy densities for the POSS cage may be used to generate an independent estimate of all $E_{i,cage}$ for every POSS compound measured. If a volume contribution for the cage can be determined, then component solubility parameters for the cage may also be estimated. By examining the consistency of the values of $E_{i,cage}$ (or the cage solubility parameters) derived from different compounds, a sense may be developed as to whether a single meaningful parameter exists, as well as a sense of what limitations are inherent to the approach.

In Table 3, the experimentally observed volumetric properties of POSS compounds are compared against values estimated by three different methods: 1) the group contribution method originally developed by Beerbower for solubility parameter estimation as expanded and reported by Hansen,[1] 2) a more recent group contribution method developed by Constantinou,[65] and 3) a "best available analog group" method described in detail in Appendix A. Although this last method relies more heavily on intuition and is not readily generalized, it is more closely linked to relevant experimental data. The experimental molar volume for POSS compounds (obtained by gas pycnometry of precipitated powder, or, in the case of octakis(hexafluoro*iso*butyl) POSS, X-ray diffraction data) was divided into a portion representing the cage (134 cc/mol, based on a model described in Appendix B) and a remainder that is assigned to the arms, with the results listed in Table 3. Note that the results of this procedure are also displayed for octa(methyl) POSS as a further check on the validity of the method.

Table 3

Calculated and Experimental Volumetric Characteristics of POSS Compounds

Arm Type	Best Available Analog Group (BAAG) relative weight)	BAAG Volume (all arms)	Beerbower GC Volume (all arms)	Constantinou GC Volume (all arms)	Estimated Arm Volume (experimental – 134 cc/mol)	Experimental Volume (source)
None	Model	134	n/a	n/a	n/a	n/a
-CH_3 x 8	n/a	n/a	252	209	226	360 (L)
-Phenethyl x 8	Ethylbenzene	845	829	868	852	986 (P)
-Styrenyl x 8	Styrene	785	787	799	827	961 (P)
-*Iso*butyl x 8	*Iso*butane	639	625	617	616	750 (P)
-Hexafluoro-*iso*butyl x 8	Hexafluoro-*iso*butylene*	924	870	n/a	743	877 (X)
-(1-naphthyl) + -Phenyl x 7	Naphthalene (1) / Benzene (7)	642	619	619	681	815 (P)

Sources: L = literature[66] ;P = pycnometry (N_2); X = x-ray crystal structure

Given the many assumptions and uncertainties involved, the agreement between the experimental and theoretical molar volume values for the arms shown in Table 3 is quite good, with the exception of octakis(hexafluoro*iso*butyl) POSS. In that case, almost all of the methods, including the experimental data, are less reliable, so the relative lack of agreement is not surprising. Moreover, no single method is clearly better or worse than the others. For calculation of the "group contribution" HSP of the cage, however, only the estimate based on experimental data is used for the volume of the cage and the arms.

Table 4 shows estimates for the cohesive energy components of the arms, again based on three theoretical methods, the best available analog group method described in Appendix A (for which a direct calculation of the energy components is employed), the Beerbower group contribution method as reported by Hansen[1] (again, for which a direct calculation of the energy components is available), and a more recent method described by Stefanis.[67] Unlike the other two methods, the Stefanis group contribution involves a calculation of group HSP, these are then multiplied by the experimental arm volume to obtain the dispersive, polar, and hydrogen bonding cohesive energy components, E_D, E_P, and E_H, respectively. The Stefanis method is available without modification for all groups needed. However, the Beerbower method is not directly applicable to the 1-naphthyl group or the fluorocarbon groups for all components. To make use of the Beerbower method, two assumptions are employed. First, the cohesive energy for the naphthyl group is calculated by scaling the values for phenyl groups

by the number of carbons (10 for naphthyl as opposed to 6 for phenyl); second, the $-CF_3$ group contribution for the polar component is calculated by taking the listed value for the total energy and subtracting the values of the other two components (which are listed as zero), even though the contribution of the polar component is listed as "?". As described in Appendix A, the best available analog group method can only generate an estimate for the dispersive component of the cohesive energy of the hexafluoro*iso*butyl group. Although a negligible contribution from hydrogen bonding to the cohesive energy density of this group represents a reasonable assumption, we have herein also used a negligible contribution from the polar component for lack of a more suitable alternative.

Table 4

Calculated Arm Group Cohesive Energies (J/cc) for POSS Compounds

Arm Type	Best Available Analog Group			Beerbower GC			Stefanis GC		
	E_D	E_P	E_H	E_D	E_P	E_H	E_D	E_P	E_H
-Phenethyl x 8	312000	350	1930	331000	1670	1670	320000	1850	10
-Styrenyl x 8	320000	930	15500	311000	2880	13700	290000	2440	100
-*Iso*butyl x 8	154000	0	0	142000	0	0	159000	2360	210
-Hexafluoro-*iso*butyl x 8	178000	? (0)	0	90400	67000	0	227000	10500	2490
-(1-Naphthyl) + -Phenyl x 7	212000	120	2650	273000	1810	1810	246000	2550	210

From Table 4, it can be seen that the agreement among the different methods is best for the phenethyl and *iso*butyl arms, and also is reasonable for the polar and hydrogen bonding components of the 1-naphthyl/phenyl arms, along with the hydrogen bonding component of the hexafluoro*iso*butyl arms. For the styrenyl arm, all three methods are in reasonable agreement for the polar component, while the best available analog group and Beerbower methods agree reasonably well for the dispersive and hydrogen bonding components, with the Stefanis method providing somewhat different estimates.

To obtain estimated group contribution HSP values for the POSS cages, the total components of the cohesive energy were calculated based on the experimental solubility parameters and molar volumes, subtracted from the calculated values for the arms, and then divided by the estimated cage volume (134 cc/mol, from Appendix B) before raising to the 0.5 power. These group contribution component

parameters are shown in Table 5 for the best available analog group method, Table 6 for the Beerbower method, and Table 7 for the Stefanis method. In Tables 5-7, a measure of the sensitivity of the calculated HSP group contributions has also been provided. The sensitivity estimate reflects the effects of assuming an error in the measurement of HSP equal to the characteristic uncertainty (explained in the Experimental section) and a simultaneous 10% error in the estimate of arm cohesive energy, with the combination always done in such a way as to augment rather than offset error. For example, an overestimate of experimental HSP, and thus total cohesive energy, is combined with a simultaneous underestimate of the cohesive energy of the arms to maximize the remaining cohesive energy assigned to the cage. Note that calculations based on the alternate analyses of the experimental data are also included in Tables 5-7.

Considering the range of previously measured HSP values, it is reassuring to note that, although in a few instances, a negative cohesive energy contribution for the cage was found, in no case is the resultant HSP value larger than 30, meaning that the estimated contributions are at least reasonable in magnitude. Moreover, particularly for the polar and hydrogen bonding components, the sensitivity is usually small. For the dispersive component, the sensitivity values are significantly larger. The greater sensitivity to error results from the fact that the dispersive energies of the system as a whole are not much different than the calculated dispersive energies of the arms. Therefore, a subtraction of two large numbers is involved to determine the dispersive component contribution of the cage. This fact, in and of itself, suggests that the dispersive component of the cage should not be drastically different than that of the arms, while the polar and hydrogen bonding components in fact should be quite large compared to the arms in all cases (with the possible exception of the polar component of the hexafluoro*iso*butyl arms).

Table 5

Calculated Group Contribution from POSS Cage Based on HSP Analysis of POSS Compounds (Beerbower Group Contributions for Arms)

Analysis Code	Calculated Cage δ_D	Sensitivity	Calculated Cage δ_P	Sensitivity	Calculated Cage δ_H	Sensitivity
PE-1	21.0	7.4	19.8	1.4	16.7	1.7
PE-A2	19.6	7.8	21.4	1.4	14.8	1.8
ST-1	24.7	7.7	14.8	2.3	14.5	2.6
IB-1	27.4	2.2	5.0	0.7	6.4	0.7
HF-1	29.3	3.7	<0	n/a	28.1	1.5
NP-1	<0	n/a	9.7	1.9	15.3	1.1
NP-A2	<0	n/a	20.9	1.8	16.1	1.0

Table 6

Calculated Group Contribution from POSS Cage Based on HSP Analysis of POSS Compounds (Stefanis Group Contributions for Arms)

Analysis Code	Calculated Cage δ_D	Sensitivity	Calculated Cage δ_P	Sensitivity	Calculated Cage δ_H	Sensitivity
PE-1	22.9	6.8	19.7	1.4	17.1	1.6
PE-A2	21.6	7.1	21.4	1.4	15.2	1.6
ST-1	27.6	6.9	15.0	2.3	17.6	1.9
IB-1	25.1	2.6	2.7	1.4	6.2	0.7
HF-1	<0	n/a	22.1	2.6	27.8	1.6
NP-1	<0	n/a	8.9	0.6	15.5	0.5
NP-A2	12.4	7.1	20.8	0.8	16.5	0.2

Table 7

Calculated Group Contributions from POSS Cage Based on HSP Analysis of POSS Compounds (Best Available Analog Group Contributions for Arms)

Analysis Code	Calculated Cage δ_D	Sensitivity	Calculated Cage δ_P	Sensitivity	Calculated Cage δ_H	Sensitivity
PE-1	24.2	6.4	20.0	1.4	16.7	1.7
PE-A2	22.9	6.7	21.6	1.4	14.7	1.7
ST-1	23.1	8.2	15.3	2.2	14.0	2.7
IB-1	25.8	2.5	5.0	0.7	6.4	0.7
HF-1	14.2	8.2	23.8	2.3	28.1	1.5
NP-1	12.3	5.9	9.8	0.5	14.9	0.6
NP-A2	20.2	4.5	21.1	0.7	15.9	0.3

As expected, extracting a meaningful cage contribution from the data on octa(hexafluoro*iso*butyl) POSS is the most problematic. The main issue, however, is not the experimental data, but rather the inability to determine a reasonable estimate of the cohesive energy components for the arms, particularly for the dispersive and polar components. For the hydrogen bonding component, the calculated values agree reasonably well with one another, but are considerably higher than those derived from measurements of the other POSS compounds. One possible explanation would be a strong electronic interaction, as suggested by X-ray data,[56] between the cage and the fluorine atoms on the arms, at least some of which must approach the cage closely due to the particular geometry of the arms.

The dispersive and polar cage contributions derived from the standard analysis of the (1-naphthyl)-heptaphenyl POSS also appear problematic. However, the alternate analysis provides values that are similar both among methods and to those found from analysis of other POSS compounds. In the case of the dispersive component, there is disagreement among the computational methods as to the contribution from the arms, with the values suggested by the Beerbower method, and to a lesser extent, the Stefanis method appearing too large. In this case, both methods have known shortcomings. The Beerbower method does not provide an explicit estimate for the naphthyl group, while the Stefanis method involves an explicit dependence of the cohesive energy density on molecular size, which is likely to result in erroneous values for larger molecules such as naphthalene. As for the polar component, the discrepancies appear to result principally from the difficulties with the standard analysis (too few good solvents by the standard criteria).

A final discrepancy is observed in the case of octa(*iso*butyl) POSS. Although all three computational methods provide similar results, the polar and hydrogen bonding components inferred from measurements of the octa(*iso*butyl) POSS are much lower than derived from the other POSS cages. Among the POSS compounds analyzed, octa(*iso*butyl) POSS conformed the least to the "spherical rule." However, the derived cage contributions appear relatively insensitive to the characteristic uncertainties in the experimental measurement. It appears as though the apparent strongly polar and hydrogen bonding character of the cage is screened by the *iso*butyl arms. Such an effect could result

from the more oblate shape of the *iso*butyl arms in comparison to the other POSS types. In fact, it does seem to be the case, based on the limited data set generated, that POSS compounds with more prolate arms (such as phenethyl, styrenyl, and (1-napthyl)heptaphenyl) provided more consistent cage contributions. Such a "prolate arm" configuration should involve less direct interaction between the cage and the arms, and thus ought to be more amenable to analysis by additive group contributions.

Despite all of the difficulties, it does appear that, at least for the prolate arm types, a "consensus" value for the cage contributions is available. As with all group contribution methods, there is a considerable amount of uncertainty. However, in many cases, group contribution methods are utilized to provide rough estimates. In these cases, the values provided by averaging the octa(phenethyl) (alternate case –A2, which appears to be slightly more precise), octa(styrenyl), and (1-napthyl)heptaphenyl alternative –A2) would seem to be provide the best estimate. For the best available analog group method, the averages are δ_D = 22 $(J/cm)^{1/2}$, δ_P = 19 $(J/cm)^{1/2}$, and δ_H = 15 $(J/cm)^{1/2}$, or, in terms of cohesive energy components, E_D = 65000 J/mol, E_P = 48000 J/mol, and E_H = 30000 J/mol. Although a characteristic uncertainty is not readily assigned to these values, based on the data in Tables 5-7, most of the values for the three compounds lie within about 5 $(J/cm)^{1/2}$ of these averages. As with any group contribution method, HSP data for many additional POSS compounds will be needed in order to transform the rough estimate provide above into a highly reliable predictive tool.

3.4 Tests of the HSP and Group Contribution Approaches for POSS Compounds

In order to truly evaluate the usefulness of the HSP approach, as well as the group contribution approach to estimating HSP, for POSS compounds, two specific tests of predictive power were performed. For HSP in general, one of the most useful predictive features is the ability to identify mixtures of non-solvents that can serve as a good solvent. Thus, guided by the calculated HSP values, we sought to identify a mixture of two poor solvents that displayed anomalously good solubility for a POSS compound. For this demonstration, we chose octa(*iso*butyl) POSS because its location on the HSP diagram and its relatively small radius of interaction provide for many possible non-solvent combinations, and because it showed a large number of exceptions to the "spherical rule", hence it

serves as a fairly stringent test of the theory. 1,4-Dioxane and n-heptane, both of which are poor solvents for octa(*iso*butyl) POSS, were chosen for the experiment. In Figure 7, quantitative solubility data for octa(*iso*butyl) POSS in mixtures of 1,4-dioxane and n-heptane are presented as a function of composition. These two non-solvents were the first fully miscible pair we tested (n-hexane and 1,1,2,2-tetrabromoethane, as well as 1-decene and quinoline, which we also attempted to test, were not fully miscible with one another).

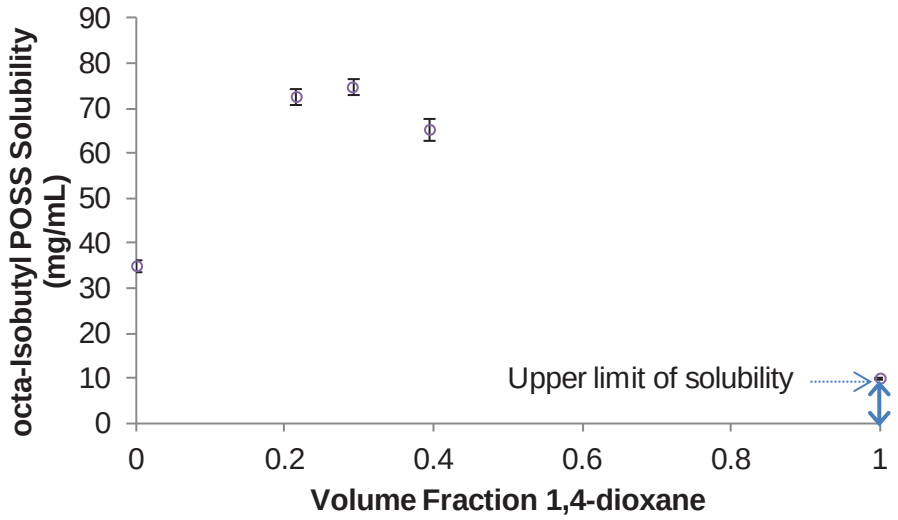

Figure 7. Solubility of octa(*iso*butyl) POSS at 20 °C as a function of 1,4-dioxane fraction in a mixed solvent system containing n-heptane and 1,4-dioxane.

As is clearly evident in Figure 7, a significant improvement in solubility is obtained when n-hexane and 1,4-dioxane are utilized as a mixed solvent system for octa(*iso*butyl) POSS. Although, strictly speaking, the most soluble mixtures fall somewhat short of the "pass" threshold of 100 mg/mL, despite the fact that they lie just within the sphere of interaction on the HSP diagram, they are more than twice as soluble as n-hexane alone and about four times as soluble as a simple rule of mixtures would predict. Moreover, the most soluble mixtures, containing 25-30 vol% 1,4-dioxane, are reasonably close in composition to the value (about 45 vol% 1,4-dioxane) that corresponds to the minimum RED for the

mixed solvent system based on the measured HSP values for octa(*iso*butyl) POSS. Thus, at a qualitative level, the predictions of HSP theory were confirmed for octa(*iso*butyl) POSS.

In order to test the group contribution approach, we again chose a stringent challenge for the theory. The compound octakis(trifluoropropyl) POSS[68] has been previously reported in studies of liquid repellent surfaces,[69] and is potentially useful as an additive to fluoropolymers. Therefore, knowledge of its HSP would have many practical benefits. Currently, however, the pure compound (containing only octameric cages) is available in extremely limited quantities, making direct measurement of its HSP using a full set of solvents impractical. Although fluoroalkyl groups pose a challenge for many group contribution approaches, general estimates of both volume and cohesive energy are still possible. The trifluoropropyl arms are also of a small, prolate shape, so cage effects should be distinguishable and the group contribution approach should be applicable. Table 8 lists the calculated volumetric, cohesive energy, and HSP data for octakis(trifluoropropyl) POSS and its components based on the three theoretical approaches outlined earlier, with details of the best available analog group method provided in Appendix A. For the Stefanis approach, calculation of the cohesive energy components requires a separate model for calculation of the molar volume. In this case, the best available analog group method was chosen, since, in cases where data on analogous compounds is readily available, it tended to predict volumes more accurately (and, unlike the case for hexafluoro*iso*butyl groups, such data is readily available for trifluoropropyl groups). For the HSP calculations, the best available analog group method is based on the best available analog group volume estimates, the Beerbower method is based on the Beerbower volume estimates, and the Stefanis method does not require a volume estimate.

Table 8. Predicted molar volume, cohesive energy, and HSP for octakis(trifluoropropyl) POSS.

Model / Parameter	Best Available Analog Group	Beerbower	Constantinou / Stefanis
Molar Volume (cc/mol)			
Each trifluoropropyl arm	79	79	n/a
Cage	134	134	134
Octakis(trifluoropropyl) POSS	766	766	n/a
Cohesive Energy (J/mol)			
Dispersive Component			
Each trifluoropropyl arm	13200	11300	19100
Cage	65000	65000	65000
Octakis(trifluoropropyl) POSS	171000	156000	217000
Polar Component			
Each trifluoropropyl arm	3940	4190	1490
Cage	48000	48000	48000
Octakis(trifluoropropyl) POSS	80000	81000	60000
Hydrogen Bonding Component			
Each trifluoropropyl arm	0	0	80
Cage	30000	30000	30000
Octakis(trifluoropropyl) POSS	30000	30000	31000
Hansen Solubility Parameters $(J/cc)^{1/2}$			
Dispersive Component			
Each trifluoropropyl arm	12.9	12.0	17.0
Cage	22	22	22
Octakis(trifluoropropyl) POSS	14.9	14.3	18.2
Polar Component			
Each trifluoropropyl arm	7.0	7.3	4.8
Cage	19	19	19
Octakis(trifluoropropyl) POSS	10.2	10.3	9.5
Hydrogen Bonding Component			
Each trifluoropropyl arm	0	0	1.1
Cage	15	15	15
Octakis(trifluoropropyl) POSS	6.3	6.3	6.9

As for the radius of interaction, there is no explicit predictive method available. However, based on the data in Tables 1 and 2, it can be seen that the radius of interaction generally increases with the size and flexibility of the arms. Also, comparing *iso*butyl and hexafluoro*iso*butyl arms, it appears that fluorination leads to an increase in the radius of interaction. The trifluoropropyl group is somewhat smaller than the *iso*butyl group, but contains limited fluorinated groups as well. If these two factors approximately counteract each other, one would expect a radius of interaction for the octakis(trifluoropropyl) POSS that is similar to the octa(*iso*butyl) POSS, or about 4.3.

In order to compare these predictions to experimental data, octakis(trifluoropropyl) POSS was dissolved in 20 test solvents. Using the predicted solubility parameters and the predicted radius of

interaction, RED values for each solvent were assigned and compared against the same "pass/fail" criteria (100 mg/mL solubility at room temperature) used for the other compounds. The results are summarized in Table 9, which shows both the experimental results and codifies the outcomes in terms of whether or not expectations were met as well as the nature of the deviations from expected behavior.

Solvent	Best Available Analog Group			Beerbower			Stefanis		
	RED	Test	Code*	RED	Test	Code*	RED	Test	Code*
1,1,2,2-tetrachloroethane	2.18	Fail	E-	2.43	Fail	E-	1.12	Fail	E-
1,4-dioxane	2.74	Fail+	E-	2.96	Fail+	E-	1.83	Fail+	E-
Acetonitrile	1.82	Fail	E-	1.85	Fail	E-	2.40	Fail	E-
Acetone	0.33	Pass	E+	0.58	Pass	E+	1.27	Pass	U+
Allyl Chloride	1.64	Fail	E-	1.83	Fail	E-	1.42	Fail	E-
Benzonitrile	1.38	Fail+	E-	1.63	Fail+	E-	0.92	Fail+	U-
Chloroform	2.14	Fail	E-	2.33	Fail	E-	1.53	Fail	E-
Cyclohexanone	1.65	Fail+	E-	1.90	Fail+	E-	0.88	Fail+	U-
Cyclopentane	2.68	Fail	E-	2.79	Fail	E-	2.64	Fail	E-
Dimethyl Formamide	1.83	Fail	E-	2.01	Fail	E-	1.46	Fail	E-
Diphenyl Ether	2.66	Fail	E-	2.90	Fail	E-	1.56	Fail	E-
Ethyl Acetate	1.23	Fail+	E-	1.37	Fail+	E-	1.48	Fail+	E-
n-Heptane	2.79	Fail	E-	2.85	Fail	E-	3.05	Fail	E-
Methyl Ethyl Ketone	0.65	Pass	E+	0.89	Pass	E+	1.11	Pass	U+
Nitrobenzene	2.46	Fail	E-	2.73	Fail	E-	1.08	Fail	E-
N,N-Dimethylacetamide	1.30	Pass	U+	1.50	Pass	U+	1.11	Pass	U+
o-Dichlorobenzene	2.30	Fail	E-	2.56	Fail	E-	1.21	Fail	E-
Propylamine	1.63	Pass	U+	1.82	Pass	U+	1.29	Pass	U+
Tetrahydrofuran	1.43	Pass	U+	1.63	Pass	U+	1.13	Pass	U+
Toluene	2.73	Fail	E-	2.92	Fail	E-	2.12	Fail	E-

*a code of "E" indicates expected behavior, while "U" indicates unexpected behavior, the "+" indicates a passing event and a "-" indicates a failing event, thus "U-" for instance, indicates an unexpected failure (i.e. lack of expected solubility).

Examining Table 9, several factors should be kept in mind. First, the group contributions for the POSS cage were derived from the data on aromatic rather than aliphatic or fluorinated POSS compounds, yet they appear to have predicted the properties of the fluoroaliphatic POSS compound quite well. Second, the differences in the performance of the three methods (with the best available analog group method and the Beerbower method appearing equally proficient) stem primarily from different predictions of the dispersive component of the fluoroalkyl arm (see Table 8), with the Stefanis method being the highest estimate. Therefore, from a group contribution standpoint, the presence of

POSS cages appears not to be a limiting factor. Some improvement in predictive capability in the case of the Stefanis method can be obtained by using a larger radius of interaction.

Based on the limited data set in Table 9, a maximization of χ^2 according to the method described in the Experimental section yields centroid parameters of δ_D = 16.9 $(J/cc)^{1/2}$, δ_P = 9.1 $(J/cc)^{1/2}$, δ_H = 8.9 $(J/cc)^{1/2}$, and R_0 = 4.5 with radii of gyration of 0.3 – 0.5 $(J/cc)^{1/2}$, five good solvents and no exceptions to the "spherical rule". Given the limited data set and the many uncertainties inherent in group contribution methods, the predicted values (which involved no adjustable parameters) agreed quite well with the experimental data. These results reinforce the earlier results that suggest the HSP approach is well-suited to POSS cages, and that group contributions for POSS cages can be utilized on at least certain types of POSS. They also illustrate that the quality of available group contribution values for the peripheral arms on POSS cages represents a major consideration when developing group contributions for the cage.

Although the present work has shown the utility of the HSP approach in understanding the solubility behavior of POSS compounds in small molecule solvents, a significantly greater payoff will be achieved if these results can be extended to POSS/polymer blends. In considering the HSP approach to predicting the miscibility of POSS compounds with polymers, there remain several important, yet unanswered questions. First, in the present work, as when determining HSP for polymers, the radius of interaction is considered a characteristic of the POSS compound rather than the solvent. For POSS/polymer blends, however, it is unclear which radius is more appropriate – that of the polymer, that of the POSS compound (which does vary significantly), or some combination of both. Second, a widely reported benefit to blending POSS compounds into polymers is the creation of free volume, which presumably results from an inability of polymer chains to penetrate the complex geometry of the POSS nanostructure. In polymer/solvent and POSS/solvent systems, the relatively small size and comparatively simple geometry of the solvent molecules allows them to "fit in" to complex geometries and mitigate these effects, but in POSS/polymer systems, the "intermeshing" of nanostructures, or lack thereof, may play a significant role in controlling miscibility. The HSP approach is not well-suited to

capturing these potentially important effects. The present work, however, by demonstrating that HSP values are a meaningful representation of cohesive energy in POSS compounds (and potentially for silicate nanostructures in general), are compatible with group contribution approaches, and have significant predictive power, effectively lays the groundwork for future investigations of these remaining issues.

4. Conclusions

Hansen Solubility Parameters (HSP) for five different Polyhedral Oligomeric SilSesquioxane (POSS) compounds have been successfully determined, demonstrating that the HSP approach developed primarily for organic compounds and polymers may be extended to at least limited types of organic-inorganic compounds. In general, the relative energy difference (i.e. "spherical rule") provided good to excellent predictive power, with somewhat less reliable predictions for octa(*iso*butyl) POSS at 100 mg/mL. Though a consistent analysis procedure was employed for all compounds, it was found that alternative analyses provided superior estimates of HSP when either the number of good solvents was very low, or when too few poor solvents were available to properly constrain the boundary of the sphere of solubility. Group contributions for the octameric POSS cage were determined using three different approaches, which gave similar results, with the best estimate being δ_D = 22 $(J/cc)^{1/2}$, δ_p = 19 $(J/cc)^{1/2}$, and δ_H = 15 $(J/cc)^{1/2}$, with an estimated uncertainty of approx. 5 $(J/cc)^{1/2}$. A major constraint in deriving and using these estimates was the ability of the various group contribution methods to correctly model the contributions from the peripheral arm groups. The utility of the HSP approach was demonstrated by successfully identifying mixtures of poor solvents that provided significantly enhanced solubility for octa(*iso*butyl) POSS, and by successfully estimating the HSP of octakis(trifluoropropyl) POSS from group contributions derived solely from aromatic POSS compounds.

Acknowledgement

Financial support for this work from the Air Force Office of Scientific Research and the Air Force Research Laboratory, Space and Missile Propulsion Division, is gratefully acknowledged. The authors

wish to thank Mr. Patrick Ruth and Ms. Amanda Wheaton of ERC Inc. for gas pycnometry, and Dr. Sean Ramirez of ERC Inc. for X-ray crystallographic data in support of this work. The octa(phenethyl) and octa(styrenyl) POSS used in this study were prepared by Dr. Rusty Blanski of AFRL, and the 1-napthylheptaphenyl POSS used in this study was prepared by Mr. Brian Moore of AFRL.

Appendix A: Description of the Best Available Analog Group Method

A1. Estimates of Molar Volume

Although many theoretical methods allow for direct estimation of the cohesive energy of a given chemical substance, certain methods, such as the group contribution approach of Stefanis,[67] involve direct calculation of solubility parameters. These methods often do not produce results that are independent of molecular size. For small molecules, these size effects must be considered, but for very large molecules, such approaches provide divergent results. A method of appropriately combining the results for smaller fragments must be developed. Because the cohesive energy is an extensive variable, it forms the natural basis for additive combination. Therefore, for large molecules, a more suitable approach is to convert the calculated solubility parameters for appropriately sized fragments into cohesive energies, add these together, and then calculate the solubility parameter for the large molecule as a whole. Such an approach was followed for POSS compounds.

The aforementioned approach requires a means of estimating the molar volume of molecular fragments. Although various correlations, such as those from Beerbower as reported by Hansen[1] and from Constantinou,[65] may be used for this purpose, they are often limited to only the most common organic chemical functionalities. In particular, as discussed in the main body of the paper, the molar volumes of naphthyl and fluoroalkyl groups found on the POSS compounds under study are not calculable using one or more of the above methods. In order to provide another basis for calculation, the “best available analog group” method was adopted. Although this method lacks a consistent set of

defined rules, it is based on straightforward principles, and can be applied to almost any chemical structure. It also has the significant advantage of being based on existing data and/or calculation.

Put simply, the "best available analog group" method involves finding the closest chemical analog of the group of interest for which either experimental data or more well-established estimates are already available, and using general rules to translate these values into new estimates. For instance, for the phenethyl group found in octa(phenethyl) POSS, the compound ethylbenzene is a close chemical analog with experimentally determined volume (and cohesive energy) values. One needs only to apply a general rule for translating the molar volume of ethylbenzene into the molar volume of the phenethyl group (an ethylbenzene with the terminal aliphatic hydrogen replaced by a chemical bond to a silicon of the POSS cage).

The effect of substituting a bond to a POSS silicon for a terminal hydrogen in general is not readily available. However, a simpler rule can be used to provide a rough estimate based on the properties of dimeric compounds. For instance, the dimer of benzene is biphenyl. Biphenyl may be visualized as consisting of two phenyl groups joined to one another, thus one means of estimating the molar volume of a phenyl group is simply to take half the molar volume of biphenyl. For many aliphatic compounds, the molar volume of the dimer is about 35 cc/mol less than twice the volume of the monomer, that is to say, the shrinkage on dimerization is about 35 cc/mol. (Numerous examples are provided in Table S4 in Supporting Information.) For a group like phenethyl, with the bonded terminal on an aliphatic group, the molar volume may be estimated as 17.5 cc/mol less than the volume of the corresponding non-bonded compound. For the phenethyl example, the molar volume estimate would be 17.5 cc/mol less than the molar volume of ethylbenzene. Note that for aromatic linkages, the shrinkage on dimerization is somewhat lower, at about 12 cc/mol.

To calculate the molar volume of a POSS compound by the "best available analog group" method, one simply needs to identify the analog group, determine the shrinkage on dimerization, and then subtract half this value from the molar volume of the analog group to estimate the volume of each arm.

The volume of the cage itself may then be added based on the model geometry estimate described in Appendix B. For all the POSS cage types studied, the shrinkage on dimerization was based on the presence of either an aliphatic or aromatic linkage at the root of each arm. For phenethyl, styrenyl, phenyl, 1-napthyl, and *iso*butyl arms, the molar volumes of the analogs (ethylbenzene, styrene, benzene, naphthalene, and *iso*butane) were all readily available. For the trifluoropropyl arm, the volume of the analog (1,1,1-trifluoropropane) is also available. For both *iso*butane and 1,1,1-trifluoropropane, the volume of the saturated liquid at 298 K (which is at higher than atmospheric pressure) was used. Note that all estimates and data sources are tabulated in Supporting Information.

For the hexafluoro*iso*butyl arm, reliable volumetric data on the analog compound 1,1,1,3,3,3-hexafluoro-2-methylpropane was not readily available. However, volumetric data for the unsaturated analog (hexafluoro*iso*butylene) was readily available. In this case, another general rule needed to be applied, based on the expected effect of hydrogenation. The expected effect of hydrogenation was determined by subtracting the molar volume of *iso*butylene from the molar volume of *iso*butane, resulting in an estimate of a 9 cc/mol increase in volume due to hydrogenation. This value was added to the experimental molar volume of hexafluoro*iso*butylene to obtain the estimated molar volume of 1,1,1,3,3,3-hexafluoro*iso*butane, which was then converted to the estimated volume of the corresponding arm by subtracting half the shrinkage on dimerization for an aliphatic group (17.5 cc/mol) to obtain the estimated arm volume. Thus, the estimated volume for the hexafluoro*iso*butyl arm is less reliable than for the arms with more common analogs, and involves certain arbitrary choices, illustrating both the strength (basis in experimental data) and weakness (lack of a straightforward universal step-by-step formula for computation) inherent in this approach.

A2. Estimates of Cohesive Energy Components

Given the complexities involved in calculating a quantity as simple as molar volumes by the “best available analog group” method, it might seem at first that calculation of cohesive energy components would be even more challenging. On the contrary, such calculations are in fact much simpler, because

the foundation of many successful group contribution methods for estimation of the molar cohesive energy is the successful assumption that it is directly proportional to the number of functional groups with only a small dependence on how those groups are arranged. For instance, the cohesive energy of the compound biphenyl is assumed to be exactly twice that of benzene in numerous group contribution methods that have proven reliable over many years. Therefore, attachment to a POSS cage can be assumed to have only a small effect on the cohesive energy of a particular arm, and thus the cohesive energy of a given arm may be assumed to equal that of its free molecule analog (e.g. the cohesive energy of a phenethyl arm is assumed to equal that of ethylbenzene). Moreover, for the purposes of the method, it is assumed that the distribution of cohesive energy components also does not change significantly with attachment to a POSS cage.

For phenethyl, styrenyl, naphthyl, and phenyl arms, experimentally derived cohesive energy components are widely available, and for computational purposes, the values provided by Hansen were used. For *iso*butyl arms, the cohesive energy components of *iso*butane were needed. In general, aliphatic hydrocarbons are assumed to have no polar or hydrogen bonding components of cohesive energy. Therefore, for *iso*butane, the total cohesive energy was determined by the thermodynamic relation

$$E = \Delta H_{vap} - RT \qquad \text{(A-1)}$$

where ΔH_{vap} is the molar heat of vaporization at 298 K, the experimental value of which was readily available, R is the universal gas constant, and T the absolute temperature. The total cohesive energy was then assumed to equal the dispersive component of the cohesive energy, with the other components being zero. Note that all estimates and data sources are tabulated in Supporting Information.

For the hexafluoro*iso*butyl arm, as mentioned previously, experimental data on the analogous compound, hexafluoro*iso*butylene, was not readily available. However, the components of cohesive energy for hexafluoro*iso*butylene, were estimated in the tables provided by Hansen.[1] As when

estimating molar volume, comparative heat of vaporization data for *iso*butylene and *iso*butane were also used to estimate the effect of hydrogenation on the dispersive component of the cohesive energy, and the difference was applied as a correction to the value for hexafluoro*iso*butylene to estimate the value for hexafluoro*iso*butane. Because the dispersive energy of organic compounds is often calculated on the basis of the total cohesive energy of the hydrocarbon homo-morph for non-fluorinated compounds, and because the difference in saturation involves a non-fluorinated portion of the molecule, the aforementioned procedure appears reasonable for the dispersive component of the cohesive energy. For the polar and hydrogen bonding components, a quick scan of cohesive energy data tables indicated that no obvious simple correction exists for comparing saturated and unsaturated compounds, so no estimation of these components was attempted for the hexafluoro*iso*butyl arm. Rather, they were simply assumed to equal zero. Note that the hydrogen bonding component of the cohesive energy for many fluorocarbons is generally assumed to equal zero in many group contribution methods as well, leaving only the polar component in question. Because fluorination of aliphatic hydrocarbons affects both dispersive and polar components of cohesive energy, the hydrocarbon homo-morph does not provide a reliable means of estimating only the dispersive component.

For the trifluoropropyl arm, cohesive energy components for 1,1,1-trifluoropropane were not readily available, though an experimental value for ΔH_{vap} at 298 K was found. The closest analog with component data estimated by Hansen is 1,1,1-trifluoroethane, although based on the NIST thermodynamic tables for 1,1,1-trifluoroethane, it appears the molar volume and solubility parameters listed are valid only at 174 K. The same NIST thermodynamic tables, however, allow for the calculation of ΔH_{vap} at 298 K. Although the distribution of cohesive energy among its components could vary somewhat with temperature, for simplicity it was assumed that the distribution remained unchanged, and the component values were simply scaled to the corrected total. Having estimated cohesive energy components for 1,1,1-trifluoroethane, it was assumed that the presence of an additional methylene group would add mainly to the dispersive component of the cohesive energy. Therefore, the

polar and hydrogen bonding components were taken to be those of 1,1,1-trifluoroethane, while the difference between their sum and the experimentally determined total based on ΔH_{vap} at 298 K was assigned to the dispersive component.

These examples illustrate, once again, the need for judicious intuition that makes the best available analog group method less attractive in some respects. In addition, it should be noted that in some cases the values for the analog compounds themselves are merely better established estimates. Therefore, while the best available analog group method has the advantage of a more direct connection to experimental data for common compounds, in cases such as fluorocarbons, where other group contribution approaches have limited success, this method also suffers from significant limitations.

Appendix B: Estimate of the Molar Volume of a POSS Cage Based on Molecular Geometry

Although it is possible to estimate the molar volume contribution of a POSS cage by comparing estimates for the arm volume with experimentally-derived total volume values, it is useful to have a theoretical comparison because the theoretical arm values contain numerous uncertain assumptions, while the experimentally-derived values are for powders of often unknown extent of crystallinity. To determine a theoretical value, the molecular geometry of the octameric POSS cage may be utilized. Although the exact details of the cage geometry differ among various compounds and are likely to change slightly based on the ordering of their surroundings, for the purposes outlined above, they are of sufficient similarity to be considered as a single entity.

In order to construct a geometric model, three forms of information are needed. The first is the relative arrangement of the centers-of-mass of each atom in the cage. Such data is readily available for X-ray studies of POSS crystals,[66] and the data for octa(methyl) POSS were chosen as a representative example. The second is the size of atoms. For this purpose, the van der Waals radii, as commonly reported, were chosen. The third, and most challenging, is an appropriate bounding shape that sets apart the region of space that “belongs to” the POSS cage.

There are many possible approaches to determining an appropriate boundary. For instance, many-atom molecular models of POSS compounds in various liquids could be constructed. From these, a Voronoi tessellation using each atom could be constructed, and the volume of the Voronoi polygons assigned to atoms of the POSS cage totaled and averaged over many models. Such an approach, though, is highly complex for the aforementioned purpose of simply providing a reasonable estimate to compare with experimental data. A much simpler approach is simply to consider the pertinent geometric factors and principles that would determine an effective boundary. The latter, simpler approach was chosen.

Although POSS compounds are known to create additional free volume in polymers and liquids, in general the packing fraction in these liquids is still expected to be close to the maximum. Therefore, any boundary should closely conform to the van der Waals radii of the cage. Although the cage itself does have certain slightly concave features, in a random arrangement of molecules, not many are likely to fit snugly into such features, and a reasonable assumption is that any boundary should define a convex interior region. Because the octameric POSS cage is approximately cubic, the simplest boundary would be a cube that circumscribed the atoms in the cage (as defined by their van der Waals radii), which equates to having an edge length of 0.684 nm. Figure B1 shows such a cube superimposed in a space-filling model of the octameric POSS cage.

The main difficulty with such a cube is that the center of mass of the peripheral carbon atom nearest to each silicon atom actually falls within the cube, so each corner of the cube contains a region that is more properly associated with the peripheral groups. To correct this issue, the cube can be truncated along a plane normal to the [111] direction (using the principal axes of the cube as principal directions). Although the plane that bisects the silicon-carbon bond seems a natural choice, one must consider that the bond length in question varies, and that the carbon atom is smaller than the silicon atom, such that the overlap of spheres defined by van der Waals radii is not centered on the bisecting plane. An "internally consistent" choice for the octameric POSS cage would be the plane that is defined by the

three points near each vertex of the cube where the van der Waals radius of the silicon atom makes contact with the cube. Although this plane is likely to pass near the center of mass of each of the nearest peripheral carbon atoms, and thus may attribute too much volume to the cage near the corners, a more accurate solution would require a concave shape in order not to exclude an inordinate amount of volume within the van der Waals radius of the silicon atoms. The location of the plane used to truncate the cube is also shown in Figure B1.

When the appropriate truncation is applied to each corner of the cube, the resultant multi-faceted shape has an appearance given by the rough sketches in Figure B2. The region is characterized by diamond-shaped faces coincident with the cube that circumscribes the cage, and by six-sided truncated triangular faces formed by the planes that truncate each corner of the cube. Figure B2 also includes a superimposed chemical structure of a portion of the cage to help clarify the relationships between the geometry of the faces and positions of the atoms in the cage. The total volume of the cube (0.3200 nm^3) equates to 192.7 cc/mol, while that of the regions excluded by truncation (0.0969 nm^3), or 58.4 cc/mol, which leaves 134 cc/mol as the volume assigned to the cage.

To check this value, the difference between the experimental volume of the POSS compounds studied and the estimated arm volume (obtained by averaging the results of the three models shown in Table 3) can be calculated. The results are: for octa(methyl) POSS, 129 cc/mol, for octa(phenethyl) POSS 139 cc/mol, for octa(styrenyl) POSS, 166 cc/mol, for octa(*iso*butyl) POSS 123 cc/mol, for (1-naphthyl)-heptaphenyl POSS, 188 cc/mol, and for octakis(hexafluoro*iso*butyl) POSS (for which the models are less reliable), -20 cc/mol. Excluding the latter, non-physical result, the average is 149 cc/mol, with a standard deviation of 27 cc/mol. Thus, the model does reasonably well in describing the experimental data. Furthermore, of the various experimental volumes calculated, the octa(methyl) POSS is likely to involve the least amount of relative error because it represents the smallest peripheral group contribution, and provides the most reliable estimate of the cage volume. From that standpoint, the model also provides a reasonable estimate.

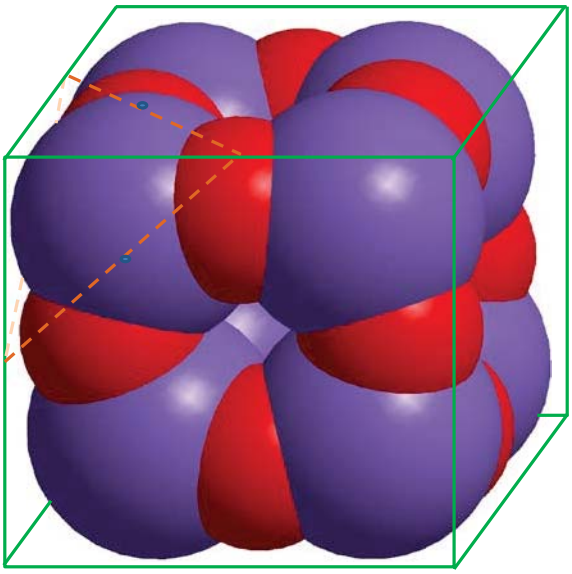

Figure B1. Key features of the geometric model of an octameric POSS cage, including circumscribing cube and the plane used to truncate the corners in order to account for the presence of peripheral groups.

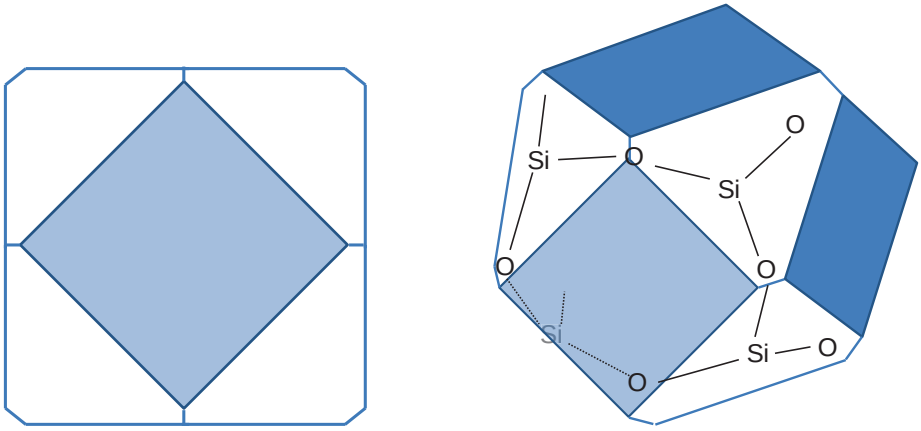

Figure B2. Sketches of the truncate cube used to define the effective volume contribution from a octameric POSS cage, including (left) view along the principal axes of the cube shown in Figure B1, and (right) rough sketch of the *iso*metric view showing the chemical structure of a portion of the cage for reference.

References

1. Hansen, C. M., *Hansen Solubility Parameters: A User's Handbook*. 2nd ed.; CRC Press: Boca Raton, FL, 2007.
2. Vink, P.; Bots, T. L. Formulation parameters influencing self-stratification of coatings. *Prog. Org. Coat.* **1996,** *28*, 173-181.
3. Hansen, C. M. 50 Years with solubility parameters - past and future. *Prog. Org. Coat.* **2004,** *51*, 77-84.
4. Hansen, C. M. Cohesion parameters for surfaces, pigments, and fillers. *JOCCA-Surf. Coat. Int.* **1997,** *80*, 386-&.
5. Hansen, C. M. The three-dimensional solubility parameter -- key to paint component affinities I. *J. Paint Technol.* **1967,** *39*, 104-117.
6. Dong, G. X.; Li, H. Y.; Chen, V. Factors affect defect-free Matrimid (R) hollow fiber gas separation performance in natural gas purification. *Journal of Membrane Science* **2010,** *353*, 17-27.
7. Hellsten, S.; Qu, H. Y.; Louhi-Kultanen, M. Screening of Binary Solvent Mixtures and Solvate Formation of Indomethacin. *Chemical Engineering & Technology* **2011,** *34*, 1667-1674.
8. Dwan'Isa, J. P. L.; Rouxhet, L.; Preat, V.; Brewster, M. E.; Arien, A. Prediction of drug solubility in amphiphilic di-block copolymer micelles: the role of polymer-drug compatibility. *Pharmazie* **2007,** *62*, 499-504.
9. Breitkreutz, J. Prediction of intestinal drug absorption properties by three-dimensional solubility parameters. *Pharm. Res.* **1998,** *15*, 1370-1375.
10. Ho, D. L.; Glinka, C. J. Effects of solvent solubility parameters on organoclay dispersions. *Chem. Mater.* **2003,** *15*, 1309-1312.
11. Li, F. H.; Bao, Y.; Chai, J.; Zhang, Q. X.; Han, D. X.; Niu, L. Synthesis and Application of Widely Soluble Graphene Sheets. *Langmuir* **2010,** *26*, 12314-12320.
12. Hansen, C. M.; Smith, A. L. Using Hansen solubility parameters to correlate solubility of C-60 fullerene in organic solvents and in polymers. *Carbon* **2004,** *42*, 1591-1597.
13. Rostami, M.; Mohseni, M.; Ranjbar, Z. Investigating the effect of pH on the surface chemistry of an amino silane treated nano silica. *Pigm. Resin. Technol.* **2011,** *40*, 363-373.
14. Schreuder, M. A.; Gosnell, J. D.; Smith, N. J.; Warnement, M. R.; Weiss, S. M.; Rosenthal, S. J. Encapsulated white-light CdSe nanocrystals as nanophosphors for solid-state lighting. *J. Mater. Chem.* **2008,** *18*, 970-975.
15. Wieneke, J. U.; Kommoss, B.; Gaer, O.; Prykhodko, I.; Ulbricht, M. Systematic Investigation of Dispersions of Unmodified Inorganic Nanoparticles in Organic Solvents with Focus on the Hansen Solubility Parameters. *Industrial & Engineering Chemistry Research* **2012,** *51*, 327-334.
16. Cordes, D. B.; Lickiss, P. D.; Rataboul, F. Recent Developments in the Chemistry of Cubic Polyhedral Oligosilsesquioxanes. *Chem. Rev.* **2010,** *110*, 2081-2173.
17. Ghanbari, H.; Cousins, B. G.; Seifalian, A. M. A Nanocage for Nanomedicine: Polyhedral Oligomeric Silsesquioxane (POSS). *Macromol. Rapid Commun.* **2011,** *32*, 1032-1046.
18. Phillips, S. H.; Haddad, T. S.; Tomczak, S. J. Developments in nanoscience: polyhedral silsesquioxane (POSS)-polymers oligomeric. *Curr. Opin. Solid State Mat. Sci.* **2004,** *8*, 21-29.
19. Hartmann-Thompson, C., *Applications of Polyhedral Oligomeric Silsesquioxanes*. Springer: New York, 2011.
20. Pakjamsai, C.; Kawakami, Y. Study on effective synthesis and properties of ortho-alkyl-substituted phenyl octasilsesquioxane. *Designed Monomers & Polymers* **2005,** *8*, 423-435.
21. Moore, B. M.; Ramirez, S. M.; Yandek, G. R.; Haddad, T. S.; Mabry, J. M. Asymmetric aryl polyhedral oligomeric silsesquioxanes (ArPOSS) with enhanced solubility. *J. Organomet. Chem.* **2011,** *696*, 2676-2680.

22. Hao, N.; Boehning, M.; Schoenhals, A. Dielectric properties of nanocomposites based on polystyrene and polyhedral oligomeric phenethyl-silsesquioxanes. *Macromolecules* **2007,** *40*, 9672-9679.
23. Iwamura, T.; Adachi, K.; Sakaguchi, M.; Chujo, Y. Synthesis of organic-inorganic polymer hybrids from poly(vinyl chloride) and polyhedral oligomeric silsesquioxane via CH/pi interaction. *Prog. Org. Coat.* **2009,** *64*, 124-127.
24. Misra, R.; Fu, B. X.; Plagge, A.; Morgan, S. E. POSS-Nylon 6 Nanocomposites: Influence of POSS Structure on Surface and Bulk Properties. *Journal of Polymer Science Part B-Polymer Physics* **2009,** *47*, 1088-1102.
25. Jones, P. J.; Cook, R. D.; McWright, C. N.; Nalty, R. J.; Choudhary, V.; Morgan, S. E. Polyhedral Oligomeric Silsesquioxane-Polyphenylsulfone Nanocomposites: Investigation of the Melt-Flow Enhancement, Thermal Behavior, and Mechanical Properties. *J. Appl. Polym. Sci.* **2011,** *121*, 2945-2956.
26. Cook, R. D.; Wei, Y. H.; Misra, R.; Morgan, S. E. Determination of polyhedral oligomeric silsesquioxane (POSS) and nylon solubility parameters for predicting dispersion in polymer composites. *Abstr. Pap. Am. Chem. Soc.* **2010,** *240*.
27. Lim, S. K.; Hong, E. P.; Song, Y. H.; Choi, H. J.; Chin, I. J. Thermodynamic interaction and mechanical characteristics of Nylon 6 and polyhedral oligomeric silsesquioxane nanohybrids. *Journal of Materials Science* **2012,** *47*, 308-314.
28. Lim, S. K.; Hong, E. P.; Choi, H. J.; Chin, I. J. Polyhedral oligomeric silsesquioxane and polyethylene nanocomposites and their physical characteristics. *J. Ind. Eng. Chem.* **2010,** *16*, 189-192.
29. Barra, J.; Pena, M. A.; Bustamante, P. Proposition of group molar constants for sodium to calculate the partial solubility parameters of sodium salts using the van Krevelen group contribution method. *European Journal of Pharmaceutical Sciences* **2000,** *10*, 153-161.
30. Bustamante, P.; Pena, M. A.; Barra, J. The modified extended Hansen method to determine partial solubility parameters of drugs containing a single hydrogen bonding group and their sodium derivatives: benzoic acid/Na and ibuprofen/Na. *Int. J. Pharm.* **2000,** *194*, 117-124.
31. Arita, T.; Moriya, K.; Yoshimura, T.; Minami, K.; Naka, T.; Adschiri, T. Dispersion of Phosphonic Acids Surface-Modified Titania Nanocrystals in Various Organic Solvents. *Industrial & Engineering Chemistry Research* **2010,** *49*, 9815-9821.
32. Chen, H. J.; Wang, L.; Chiu, W. Y. Chelation and solvent effect on the preparation of titania colloids. *Mater. Chem. Phys.* **2007,** *101*, 12-19.
33. Lafaurie, A.; Azema, N.; Ferry, L.; Lopez-Cuesta, J. M. Stability parameters for mineral suspensions: Improving the dispersion of fillers in thermoplastics. *Powder Technol.* **2009,** *192*, 92-98.
34. Shibata, J.; Fujii, K.; Horai, K.; Yamamoto, H. Dispersion and flocculation behavior of metal oxide powders in organic solvent. *Kag. Kog. Ronbunshu* **2001,** *27*, 497-501.
35. Shibata, J.; Fujii, K.; Yamamoto, H. Dispersion and flocculation behavior of rare earth oxide powders in organic solvent. *Kag. Kog. Ronbunshu* **2002,** *28*, 641-646.
36. Klingenfus, J.; Palmas, P. Weak molecular associations investigated by (1)H-NMR spectroscopy on a neat organosiloxane-solvent mixture. *PCCP* **2011,** *13*, 10661-10669.
37. Schierholz, J. M. Physico-chemical properties of a rifampicin-releasing polydimethylsiloxane shunt. *Biomaterials* **1997,** *18*, 635-641.
38. Zhou, H. L.; Su, Y.; Chen, X. R.; Wan, Y. H. Separation of acetone, butanol and ethanol (ABE) from dilute aqueous solutions by silicalite-1/PDMS hybrid pervaporation membranes. *Sep. Purif. Technol.* **2011,** *79*, 375-384.
39. Orme, C. J.; Klaehn, J. R.; Harrup, M. K.; Lash, R. P.; Stewart, F. F. Characterization of 2-(2-methoxyethoxy)ethanol-substituted phosphazene polymers using pervaporation, solubility parameters, and sorption studies. *J. Appl. Polym. Sci.* **2005,** *97*, 939-945.
40. Cataldo, F. On the Solubility Parameter of C60 and Higher Fullerenes. *Fuller. Nanotub. Carbon Nanostruct.* **2009,** *17*, 79-84.

41. Acevedo, S.; Castro, A.; Vasquez, E.; Marcano, F.; Ranaudo, M. A. Investigation of Physical Chemistry Properties of Asphaltenes Using Solubility Parameters of Asphaltenes and Their Fractions A1 and A2. *Energy & Fuels* **2010,** *24*, 5921-5933.
42. Aray, Y.; Hernandez-Bravo, R.; Parra, J. G.; Rodriguez, J.; Coll, D. S. Exploring the Structure-Solubility Relationship of Asphaltene Models in Toluene, Heptane, and Amphiphiles Using a Molecular Dynamic Atomistic Methodology. *J. Phys. Chem. A* **2011,** *115*, 11495-11507.
43. Mutelet, F.; Ekulu, G.; Solimando, R.; Rogalski, M. Solubility parameters of crude oils and asphaltenes. *Energy & Fuels* **2004,** *18*, 667-673.
44. Nikooyeh, K.; Shaw, J. M. On the Applicability of the Regular Solution Theory to Asphaltene plus Diluent Mixtures. *Energy & Fuels* **2012,** *26*, 576-585.
45. Redelius, P. Bitumen solubility model using Hansen solubility parameter. *Energy & Fuels* **2004,** *18*, 1087-1092.
46. Wang, T.; Zhang, Y. Z. Methods for Determining the Solubility Parameter of Bitumen. *J. Test. Eval.* **2010,** *38*, 383-389.
47. Hao, N.; Bohning, M.; Schonhals, A. CO(2) Gas Transport Properties of Nanocomposites Based on Polyhedral Oligomeric Phenethyl-Silsesquioxanes and Poly(bisphenol A carbonate). *Macromolecules* **2010,** *43*, 9417-9425.
48. Voronkov, M. G.; Kovrigin, V. M.; Lavrent'ev, V. I.; Moralev, V. M. Reaction of pervinyloctasilsesquioxane with benzene in the presence of aluminum trichloride. Perphenethyloctasilsesquioxane. *Dokl. Akad. Nauk SSSR* **1985,** *281* (6).
49. Sanchez-Soto, M.; Schiraldi, D. A.; Illescas, S. Study of the morphology and properties of melt-mixed polycarbonate-POSS nanocomposites. *Eur. Polym. J.* **2009,** *45*, 341-352.
50. Hosaka, N.; Otsuka, H.; Hino, M.; Takahara, A. Control of dispersion state of silsesquioxane nanofillers for stabilization of polystyrene thin films. *Langmuir* **2008,** *24*, 5766-5772.
51. Hao, N.; Bohning, M.; Goering, H.; Schonhals, A. Nanocomposites of polyhedral oligomeric phenethylsilsesquioxanes and poly(bisphenol A carbonate) as investigated by dielectric spectroscopy. *Macromolecules* **2007,** *40*, 2955-2964.
52. Blanski, R. L.; Phillips, S. H.; Chaffee, K.; Lichtenhan, J.; Lee, A.; Geng, H. P., Preparation and properties of organic-inorganic hybrid materials by blending polyhedral oligosilsesquioxanes into organic polymers. *Polymer Preprints* **2000,** *41*, 585-586.
53. Blanski, R. L.; Phillips, S. H.; Chaffee, K.; Lichtenhan, J.; Lee, A.; Geng, H. P. The Synthesis of Hybrid Materials by the Blending of Polyhedral Oligosilsesquioxanes into Organic Polymers. *Mater. Res. Soc. Symp. Proc.* **2000,** *628*, CC6.27.1 - CC6.27.6.
54. Feher, F. J.; Soulivong, D.; Eklund, A. G.; Wyndham, K. D., Cross-metathesis of alkenes with vinyl-substituted silsesquioxanes and spherosilicates: A new method for synthesizing highly-functionalized Si/O frameworks. *Chem. Commun.* **1997**, 1185-1186.
55. Chhatre, S. S.; Guardado, J. O.; Moore, B. M.; Haddad, T. S.; Mabry, J. M.; McKinley, G. H.; Cohen, R. E. Fluoroalkylated Silicon-Containing Surfaces-Estimation of Solid-Surface Energy. *ACS Applied Materials & Interfaces* **2010,** *2*, 3544-3554.
56. Mabry, J. M.; Vij, A.; Iacono, S. T.; Viers, B. D. Fluorinated polyhedral oligomeric silsesquioxanes (F-POSS). *Angew. Chem., Int. Ed.* **2008,** *47*, 4137-4140.
57. Tuteja, A.; Choi, W.; Ma, M. L.; Mabry, J. M.; Mazzella, S. A.; Rutledge, G. C.; McKinley, G. H.; Cohen, R. E. Designing superoleophobic surfaces. *Science* **2007,** *318*, 1618-1622.
58. Belmares, M.; Blanco, M.; Goddard, W. A.; Ross, R. B.; Caldwell, G.; Chou, S. H.; Pham, J.; Olofson, P. M.; Thomas, C. Hildebrand and Hansen solubility parameters from molecular dynamics with applications to electronic nose polymer sensors. *J. Comput. Chem.* **2004,** *25*, 1814-1826.
59. Choi, P.; Kavassalis, T. A.; Rudin, A. Estimation of Hansen Solubility Parameters for (Hydroxyethyl)-Cellulose and (Hydroxypropyl)Cellulose through Molecular Simulation. *Industrial & Engineering Chemistry Research* **1994,** *33*, 3154-3159.

60. Jarvas, G.; Quellet, C.; Dallos, A. Estimation of Hansen solubility parameters using multivariate nonlinear QSPR modeling with COSMO screening charge density moments. *Fluid Phase Equilib.* **2011,** *309*, 8-14.
61. Tantishaiyakul, V.; Worakul, N.; Wongpoowarak, W. Prediction of solubility parameters using partial least square regression. *Int. J. Pharm.* **2006,** *325*, 8-14.
62. Zeng, F. L.; Sun, Y.; Zhou, Y.; Li, Q. K. Molecular simulations of the miscibility in binary mixtures of PVDF and POSS compounds. *Modell. Simul. Mater. Sci. Eng.* **2009,** *17* (7).
63. Zeng, Z. Y.; Xu, Y. Y.; Li, Y. W. Calculation of Solubility Parameter Using Perturbed-Chain SAFT and Cubic-Plus-Association Equations of State. *Industrial & Engineering Chemistry Research* **2008,** *47*, 9663-9669.
64. Stefanis, E.; Tsivintzelis, I.; Panayiotou, C. The partial solubility parameters: An equation-of-state approach. *Fluid Phase Equilib.* **2006,** *240*, 144-154.
65. Constantinou, L.; Gani, R.; Oconnell, J. P. Estimation of the acentric factor and the liquid molar volume at 298-k using a new group-contribution method. *Fluid Phase Equilib.* **1995,** *103*, 11-22.
66. Larsson, K., The crystal structure of octa-(methylsilsesquioxane) (CH-sub-3-SiO-sub-1.5)-sub-8. *Ark. Kemi* **1960,** *16*, 203-208.
67. Stefanis, E.; Panayiotou, C. Prediction of Hansen solubility parameters with a new group-contribution method. *Int. J. Thermophys.* **2008,** *29*, 568-585.
68. Lavrent'ev, V. I. Per(gamma-trifluoropropyl)octasilsesquioxane. *Russ. J. Gen. Chem.* **2004,** *74*, 1188-1193.
69. Iacono, S. T.; Vij, A.; Grabow, W.; Smith, D. W.; Mabry, J. M., Facile synthesis of hydrophobic fluoroalkyl functionalized silsesquioxane nanostructures. *Chem. Commun.* **2007**, 4992-4994.

Supporting Information

"Hansen Solubility Parameters for Octahedral Oligomeric Silsesquioxanes"

Andrew J. Guenthner[1]*, *Kevin R. Lamison*[2], *Lisa M. Lubin*[2], *Timothy S. Haddad*[2], *Joseph M. Mabry*[1]

[1]Propulsion Directorate, Air Force Research Laboratory, Edwards AFB, CA 93524
[2]ERC Incorporated, Edwards AFB, CA 93524

*andrew.guenthner@edwards.af.mil

Table S1 lists the names of all 45 solvents used in the "standard" test set for determination of the Hansen Solubility Parameters (HSP) of five octameric POSS compounds, octa(phenethyl), octa(styrenyl), octa(*iso*butyl), octa(hexafluoro*iso*butyl), and (1-naphthyl)-heptaphenyl POSS. Note that due to limited supplied of material, only 36 of the 45 solvents were used with octa(hexafluoro*iso*butyl) POSS. Table 1 provides both the test results and whether or not those results agree with the "spherical rule" based on the subsequent HSP determination. Details of the experiments, the ratings, and the HSP determination procedure may be found in the main body of the paper. "Pass" indicates total dissolution within two minutes, "Pass –" indicates total dissolution within two minutes to one hour, "Fail" indicates no dissolution whatsoever, and "Fail+" indicates incomplete dissolution with some visible signs of good dispersion or partial dissolution. Note that results of the "Supplemental" testing are listed in Table S2 (see the main body of the text for a detailed description of supplemental tests). Briefly, whereas the "standard" tests were carried out at 100 mg/mL, test PE-A1 utilized 200 mg/mL, and test NP-A1 utilized 50 mg/mL. Test PE-A2 utilized additional solvents and solvent mixtures, listed in Table S3.

Table S1

Solubility Test Results for "Standard" Tests

Solvent	PE		ST		IB		HF		NP	
	P/F	E/U	P/F	E/U	P/F	E/U	P/F	E/U	P/F	E/U
1,1,2,2-Tetrabromoethane	P-	E	F+	U	F+	E	F	E	F	E
1,1,2,2-Tetrachloroethane	P	E	P	E	P-	E	F	E	F+	E
1,4-Butanediol	F	E	F	E	F	E	F	E	F	E
1,4-Dioxane	P-	E	F	U	F+	E	F	E	F	E
1-Decene	F+	E	F	E	F	E			F	E
2-Chlorophenol	P	E	P	E	F	E			F	E
2-Ethyl-1-hexanol	F+	E	F	E	F	E			F	E
Acetonitrile	F	E	F	E	F	E	F	E	F	E
Acetone	P	E	F+	E	F+	E	P	E	F	E
Allyl chloride	P	E	P	E	F	E	F	E	F	E
Benzene	P	E	P	E	F+	U			F	E
Benzonitrile	P	E	P-	E	P	E	F	E	F+	E
Benzyl chloride	P	E	P	E	P	E	F	E	F	E
Chloroform	P	E	P	E	P	E	F	E	P	E
Cyclohexane	P-	U	F	E	P	E	F	E	F	E
Cyclohexanone	P	E	F+	U	F+	E	F	E	F+	E
Cyclopentane	F+	E	F	E	P	E	F	E	F	E
Diethyl ether	P	U	F	E	P	U	F	E	F	E
Dimethyl Formamide	P-	E	P	E	F	E	P	E	F	E
Dimethyl Sulfoxide	F	E	F	E	F	E	F	E	F	E
Di-n-butyl ether	F+	E	F	E	F	E			F	E
Diphenyl Ether	P-	E	P-	E	F+	E	F	E	F+	E
Dodecane	F+	E	F	E	F+	E			F	E
Ethanol	F	E	F	E	F	E	F	E	F	E
Ethyl Acetate	P	E	P	E	F	E	P	E	F	E
EGDE	P	E	P	E	F	E	P	E	F	E
n-Heptane	F	E	F	E	F	E	P	U	F	E
Hexadecane	F	E	F	E	F+	E			F	E
Isopropanol	F	E	F	E	F	E	F	U	F	E
Methyl Ethyl Ketone	P	E	P	E	F	E	P	E	F	E
n-Butanol	F	E	F	E	F	E	P	E	F	E
n-Hexane	F	E	F	E	P	U	F	E	F	E
Nitrobenzene	P	E	P	E	F+	E	F	E	F	E
N-methyl-2-pyrrolidone	P	E	P	E	F+	E			P	U
N-N-dimethylacetamide	P	E	F+	U	F+	E	P	E	F	E
n-Propanol	F	E	F	E	F	E	P	E	F	E
o-Dibromobenzene	P	E	P-	E	F	E			F	E
o-Dichlorobenzene	P	E	F	U	F+	E	F	E	F	E
Phenyl acetylene	P	E	P	E	F	U	F	E	F	E
Propylamine	P	E	P	E	F	E	P	E	F	E

Solvent	PE		ST		IB		HF		NP	
	P/F	E/U	P/F	E/U	P/F	E/U	P/F	E/U	P/F	E/U
Propylene Carbonate	F+	E	F	E	F	E	F	E	F	E
Quinoline	P-	E	P	E	F	E	F	E	F	E
Tetrahydrofuran	P	E	P	E	P	U	P	E	P	E
Toluene	P	E	P	E	P-	E	F	E	F	E
Xylenes	P	E	P-	E	F+	U	F	E	F	E

Guide to abbreviations:
EGDE: ethylene glycol dimethyl ether
PE: octa(phenethyl) POSS
ST: octa(styrenyl) POSS
IB: octa(*iso*butyl) POSS
HF: octakis(hexafluoro*iso*butyl) POSS
NP: (1-naphthyl)heptaphenyl POSS
E: as expected, based on best fit HSP and “spherical rule”
U: not as expected, based on best fit HSP and “spherical rule”

Table S2

Solubility Test Results for "Supplemental" Tests

Solvent	PE-A1		NP-A1		NP-A2	
	P/F	E/U	P/F	E/U	P/F	E/U
1,1,2,2-Tetrabromoethane	P	E	F	E	F	E
1,1,2,2-Tetrachloroethane	P	E	F+	E	F+*	E
1,4-Butanediol	F	E	F	E	F	E
1,4-Dioxane	P	E	F	E	F	E
1-Decene	F+	E	F	E	F	E
2-Chlorophenol	F	U	F	E	F	E
2-Ethyl-1-hexanol	F+	E	F	E	F	E
Acetonitrile	F	E	F	E	F	E
Acetone	F	E	F	E	F	E
Allyl chloride	F	E	F	E	F	E
Benzene	F+	E	F	E	F	E
Benzonitrile	P	E	F+	E	F+*	E
Benzyl chloride	P	E	F	E	F	E
Chloroform	P	E	P	E	P	U
Cyclohexane	F	E	F	E	F	E
Cyclohexanone	P	E	F+	E	F+*	E
Cyclopentane	F	E	F	E	F	E
Diethyl ether	F+	E	F	E	F	E
Dimethyl Formamide	P	E	F	E	F	E
Dimethyl Sulfoxide	F	E	F	E	F	E
Di-n-butyl ether	F+	E	F	E	F	E
Diphenyl Ether	F	U	F+	E	F+*	U
Dodecane	F+	E	F	E	F	E
Ethanol	F	E	F	E	F	E
Ethyl Acetate	F	E	F	E	F	E
EGDE	F	E	F	E	F	E
n-Heptane	F	E	F	E	F	E
Hexadecane	F	E	F	E	F	E
Isopropanol	F	E	F	E	F	E
Methyl Ethyl Ketone	F	E	F	E	F	E
n-Butanol	F	E	F	E	F	E
n-Hexane	F	E	F	E	F	E
Nitrobenzene	P-	E	F	E	F	E
N-methyl-2-pyrrolidone	P-	E	P	U	P	E
N-N-dimethylacetamide	P-	E	F	E	F	E
n-Propanol	F	E	F	E	F	E
o-Dibromobenzene	P	E	F	E	F	E
o-Dichlorobenzene	P	E	F	E	F	E
Phenyl acetylene	P	E	F	E	F	E
Propylamine	P	E	F	E	F	E

Solvent	PE-A1		NP-A1		NP-A2	
	P/F	E/U	P/F	E/U	P/F	E/U
Propylene Carbonate	F	E	F	E	F	E
Quinoline	P	E	F	E	F	E
Tetrahydrofuran	P	E	P	E	P	E
Toluene	P	E	F	E	F	E
Xylenes	P	E	F	E	F	E

Abbreviations as in Table S1.
* Note that for analysis NP-A2, ratings of "Fail+" were treated as "Pass"

Table S3

Additional Solvents and Solvent Mixtures for Test PE-A2

Solvent	PE-A2	
	P/F	E/U
Allyl alcohol	F	E
Nonylphenol	P-	E
Acetonitrile / benzonitrile 87 / 13 v / v	F	E
Acetonitrile / benzonitrile 77 / 23 v / v	P-	U
Acetonitrile / benzonitrile 52 / 48 v / v	P-	E
Acetonitrile / isopropanol 54 / 46 v / v	F+	E
Acetonitrile / n-butanol 53 / 47 v / v	F	E
n-Butanol / propylamine 80 / 20 v / v	F	E
Nitrobenzene / propylene carbonate 52 / 48 v / v	P-	E
Nitrobenzene / propylene carbonate 22 / 78 v / v	F	E
o-Dichlorobenzene / propylene carbonate 60 / 40 v / v	P	E
Quinoline / 1,1,2,2,-Tetrabromoethane 52 / 48 v / v	P	E

Abbreviations as in Table S1. Note that the expected / unexpected behavior for the other solvents included in analysis PE-A2 did not change from that found for the standard analysis.

The following Tables (S4 – S6) provide the sources and values for molar volume and cohesive energy calculations carried out using the "best available analog group" method. The method is explained in detail in Appendices A.1 (molar volume) and A.2 (cohesive energy) in the main body of the paper.

Table S4

Examples Used for Estimating the Shrinkage on Dimerization

Monomer Name	Molar Volume (cc/mol) at 25 °C	Source ID	Dimer Name	Dimer Volume (cc/mol) at 25 °C	Source ID	Shrinkage on Dimer-ization (cc/mol)[a]	Correction to Monomer Volume (cc/mol)[b]
n-Butane	100.4	1b	n-Octane	163.5	1b	37.3	18.6
n-Pentane	116.2	1b	n-Decane	195.9	1b	36.5	18.2
n-Hexane	131.6	1a	n-Dodecane	228.6	1b	34.6	17.3
n-Heptane	147.4	1b	n-Tetradecane	261.3	1b	33.5	16.8
n-Octane	163.5	1b	n-Hexadecane	294.1	1b	32.9	16.4
Benzene	89.4	1a	Biphenyl	155.1	1b	23.7	11.8
Isobutane	98.1[c]	2	2,5-Dimethyl-hexane	165	3	31	16
1-Chloro-butane	105	3	1,8-Dichloro-octane	178[d]	4	32	16

Notes: a. That is, twice the volume of the monomer minus the volume of the dimer

b. That is, the amount subtracted from the monomer volume used to estimate the volume of the attached group, e.g. a hexyl group would be 17.3 cc/mol smaller than hexane.

c. at 15 °C

d. at 20 °C

Source IDs:

1a. Hansen, C. M., *Hansen Solubility Parameters: A User's Handbook*. 2nd ed.; CRC Press: Boca Raton, FL, 2007; Table A.1 (experimental value)

1b. Hansen, C. M., *Hansen Solubility Parameters: A User's Handbook*. 2nd ed.; CRC Press: Boca Raton, FL, 2007; Table A.1 (calculated value)

2. Air Liquide Product Data Sheet

3. Sigma-Aldrich Product Data Sheet\

4. Merck Product Data Sheet

Table S5
Estimates of Molar Volume by Best Available Analog Group Method

Group	Analog	Analog Molar Volume (cc/mol) at 25 °C	Source ID	Correction Applied (cc/mol)	Estimated Group Molar Volume (cc/mol) at 25 °C
-Phenethyl	Ethylbenzene	123.1	1a	17.5	105.6
-Styrenyl	Styrene	115.6	1a	17.5	98.1
-Phenyl	Benzene	89.4	1a	12	77.4
-1-Naphthyl	Naphthalene	111.5	1b	12	99.5
-Isobutyl	Isobutane	98.1[a]	2	17.5	80.6
-Hexafluoro-isobutyl	Hexafluoroisobutylene	124	3	8.5[b]	115.5
-Trifluoro-propyl	1,1,1-Trifluoropropane	96.9	4	17.5	79.4

Notes: a: at 15 °C
b. Based on applying both the dimerization correction of 17.5 cc/mol, and an additional correction for hydrogenation, equal to the difference between the molar volumes of isobutane (98.1 cc/mol at 15 °C from source 2) and isobutylene (89.4 cc/mol at 25 °C from source 1b), or 9 cc/mol).

Source IDs:
1a. Hansen, C. M., *Hansen Solubility Parameters: A User's Handbook*. 2nd ed.; CRC Press: Boca Raton, FL, 2007; Table A.1 (experimental value)
1b. Hansen, C. M., *Hansen Solubility Parameters: A User's Handbook*. 2nd ed.; CRC Press: Boca Raton, FL, 2007; Table A.1 (calculated value)
2. Air Liquide Product Data Sheet
3. DuPont Product Data Sheet
4. Mattox, D. M. *The Foundations of Vacuum Coating Technology*; Noyes / William Andrew Publishing: Norwich, NY, 2003.

Table S6

Estimates of Cohesive Energy by Best Available Analog Group Method

Group	Analog	Analog Cohesive Energy (J/mol) at 25 °C			Source ID
		Dispersive	Polar	H-Bonding	
-Phenethyl	Ethylbenzene	39000	40	240	1a
-Styrenyl	Styrene	40000	120	1900	1a
-Phenyl	Benzene	30000	0	360	1a
-1-Naphthyl	Naphthalene	41000	450	3900	1b
-Isobutyl	Isobutane	19000[a]	0	0	2
-Hexafluoroisobutyl	Hexafluoroisobutylene	22000[b]	0	0	3
-Trifluoropropyl	1,1,1-Trifluoropropane	13000[c]	3900[d]	0[d]	1b,4,5

Notes: a. based on ΔH_{vap} at 25 °C

b. Based on ΔH_{vap} at 25 °C determined from the Clausius-Clapeyron form of the listed vapor pressure data, assumed entirely dispersive, and a correction for hydrogenation, equal to the difference between the dispersive cohesive energies of isobutane (1,9200 J/mol at 15 °C from source 2) and isobutylene (18,800 J/mol at 25 °C from source 1b), or 400 J/mol).

c. Based on the total (from ΔH_{vap} at 25 °C reported in source 4) minus the expected polar and hydrogen-bonding contributions

d. The values for the polar and H-bonding cohesive energies are taken from those reported in source 1b for 1,1,1-trifluoroethane, corrected for temperature by scaling the computed values of E_{coh} (based on ΔH_{vap}) at an assumed 174 K (from source 1b) to that at 298 K (from source 5), Note that the values reported in source 5 at 174 K match those reported in source 1b, both for molar volume and ΔH_{vap}. These values are assumed not to be altered by addition of a methylene group.

Further explanation:

According to source 1b, E_{coh} for 1,1,1-trifluoroethane is 21,200 J/mol, with E_D = 13,800 J/mol and E_P = 7,400 J/mol. Accounting for PV yields ΔH_{vap} = 22,600 J/mol. According to source 5, ΔH_{vap} at 174 K equals approximately this value, however, at 298 K (making use of the thermodynamic tables), ΔH_{vap} = 13,700 J/mol, or, equivalently, E_{coh} = 11,300 J/mol. Hence, the component values from source 1b have been scaled by the factor (11,300) / (21,200), resulting in estimates of E_D = 7,400 J/mol and E_P = 3,900 J/mol at 298 K for 1,1,1-trifluoroethane.

For 1,1,1-trifluoropropane, the value of ΔH_{vap} at 298 K from source 4 is 19,600 J/mol, or E_{coh} = 17,100 J/mol after accounting for PV. In order to estimate components, it is assumed that the dipoles in 1,1,1-trifluoropropane are simply diluted versions of the dipoles in 1,1,1-trifluoroethane, hence E_P is assumed equal for both compounds, at 3,900 J/mol. It is assumed that E_H also remains zero, hence the remaining 13,200 J/mol is assigned to E_D.

Source IDs:

1a. Hansen, C. M., *Hansen Solubility Parameters: A User's Handbook*. 2nd ed.; CRC Press: Boca Raton, FL, 2007; Table A.1 (experimental value)

1b. Hansen, C. M., *Hansen Solubility Parameters: A User's Handbook*. 2nd ed.; CRC Press: Boca Raton, FL, 2007; Table A.1 (calculated value)

2. *CRC Handbook of Chemistry and Physics, 82nd ed.* (D. R. Lide, ed.); CRC Press: Boca Raton, FL, 2001; p. 6-113.
3. DuPont Product Data Sheet
4. Mattox, D. M. *The Foundations of Vacuum Coating Technology*; Noyes / William Andrew Publishing: Norwich, NY, 2003.
5. NIST/TRC Web Thermo Tables (WTT); available online at http://webbook.nist.gov/cgi/fluid.cgi?ID=C420462&Action=Page, with additional information available at http://wtt-lite.nist.gov/wtt-lite/index.html?cmp=1.1.1-trifluoroethane, accessed March 1, 2012.